U.PORTO

MESTRADO
MEDICINA E ONCOLOGIA MOLECULAR

The Effect of Anti-Diabetic Drugs on the Metabolism of Papillary Thyroid Cancer

Miguel Soares Castanho

M

2025

Miguel Soares Castanho

The Effect of Anti-Diabetic Drugs on the Metabolism of Papillary Thyroid Cancer

Dissertação de Candidatura ao grau de **Mestre em Medicina e Oncologia Molecular** submetida à Faculdade de Medicina da Universidade do Porto

Orientador: **Professor Valdemar de Jesus Conde Máximo**
Professor Associado
Faculdade de Medicina da Universidade do Porto, Universidade do Porto
Investigador Principal
Grupo Cancer Signalling and Metabolism
Instituto de Investigação e Inovação em Saúde da Universidade do Porto
Instituto de Patologia e Imunologia Molecular da Universidade do Porto

Coorientadora: **Professora Ana Paula Soares Dias Ferreira**
Professora Associada
Faculdade de Medicina da Universidade do Porto, Universidade do Porto
Investigadora Coordenadora
Grupo Cancer Signalling and Metabolism
Instituto de Investigação e Inovação em Saúde da Universidade do Porto
Instituto de Patologia e Imunologia Molecular da Universidade do Porto

This study is partially supported by the Norte Portugal Regional Operational Programme (NORTE 2020) under the PORTUGAL 2020 Partnership Agreement through the European Regional Development Fund (ERDF) and the project “The Porto Comprehensive Cancer Center” ref. NORTE-01-0145-FEDER-072678—Consórcio PORTO.CCC—Porto, Comprehensive Cancer Center Raquel Seruca.

This study was partially supported by the grant “Papel dos fármacos antidiabéticos no carcinoma diferenciado da tiroide: implicações da modulação do metabolismo energético na fisiopatologia e terapêutica do carcinoma papilar da tiroide” (ADCPT, funded by the Sociedade Portuguesa de Endocrinologia, Diabetes e Metabolismo (SPEDM)).

AGRADECIMENTOS

Quando comecei a minha vida académica, já tinha definido como objetivo final para esta fase este momento. No entanto, nada me podia ter preparado para todo o trajeto que percorri desde a licenciatura, passando pelo mestrado e pelo grupo Cancer Signalling and Metabolism, onde desenvolvi esta dissertação. Ao longo deste percurso, cheio de surpresas, cresci como estudante, como investigador e principalmente como pessoa. E como nenhum caminho se faz sozinho, deixo os meus agradecimentos às pessoas mais importantes desta fase do meu desenvolvimento:

Ao Professor Valdemar, o meu orientador, por me ter confiado a responsabilidade de assumir um papel ativo neste projeto. Obrigado por ter sempre a porta aberta para esclarecer as muitas dúvidas que foram surgindo ao longo do trajeto e por me ter sempre encaminhado da melhor forma quando os resultados não eram os esperados.

À Professora Paula, minha coorientadora e group leader, por me ter recebido no grupo com toda a disponibilidade desde o primeiro dia. Obrigado por me permitir ter a honra de ser um membro deste grupo tão prestigiado e de trabalhar lado a lado com pessoas que admiro.

Um muito obrigado a todos os membros do grupo Cancer Signalling and Metabolism, por me terem acolhido nesta equipa incrível que se foi transformando numa segunda família. Um agradecimento especial à Elisa, por ter sempre um conselho sábio quando parece que o trabalho está perdido, ao Tito, por ser o pronto-socorro quando nada está a bater certo no laboratório, e ao Arnaud, por me ter aberto as portas a novas oportunidades na área fascinante da Bioinformática.

Estendo o agradecimento a todos os técnicos e auxiliares do I3S, cujo trabalho me permitiu ter todas as condições para realizar este projeto. Agradeço particularmente ao Rui Fernandes e à Sofia Pacheco da plataforma HEMS, ao André Maia da plataforma Bioscreening e ao Hugo Osório da plataforma Proteomics.

Queria também agradecer a todos os docentes e não-docentes da FCUP, ICBAS, SZTE e FMUP por terem contribuído para a minha formação académica ao longo dos últimos 6 anos e terem confirmado que a Ciência é onde eu quero estar.

À Lia, a minha "irmã mais velha", apesar de nem sempre se perceber quem é o mais velho, a minha companheira de horas de almoço ou chill outs, trabalho nas células ou idas ao armazém, lanches ou finos. Obrigado por teres estado sempre lá para mim, nos momentos de festa, mas principalmente nos momentos em que só precisava de tirar um peso de cima dos ombros. Conhecer-te foi sem dúvida um dos highlights deste percurso, que poderia não ser pior, mas de certeza que tinha muito menos piada sem ti ao lado.

À Patrícia, só tenho a agradecer por os nossos caminhos se terem voltado a cruzar. Obrigado por teres perdido tanto tempo a facilitar o meu trabalho neste último ano, por todos os conselhos, pela paixão e força de vontade que demonstras diariamente e que servem de exemplo para todos. Foste uma peça indispensável do meu percurso, começando na licenciatura e terminando onde quer que seja que os nossos caminhos se cruzarão a seguir, mal posso esperar!

À Gabi, a minha "irmã mais nova", por todos os dias ouvir o que eu tenho para dizer, quer sejam conselhos, desabafos ou momentos em que mais valia estar calado. Obrigado por me teres carregado pelos momentos de maior desânimo no laboratório e por teres sempre uma história pronta para animar qualquer momento.

Ao Rui e à Bia, antes de mais por serem a minha porta de entrada para o grupo, mas também por se terem tornado muito mais que isso ao longo do tempo. Ao Rui, obrigado por seres uma fonte de apoio e motivação ao longo de todo este projeto e por todas as boleias e histórias que partilhaste comigo. À Bia, obrigado por (quase) todos os dias seres a luz que ilumina todo o laboratório e torna tudo mais fácil, mas também, e talvez ainda mais, por me teres deixado entrar nos dias em que a luz não está acesa. As nossas deep talks ao longo do ano foram momentos-chave do meu percurso e espero que tenha conseguido ajudar da mesma forma como me ajudaste a mim.

À Inês, a minha parceira de licenciatura desde o dia 1, com quem partilhei aulas e jantares, reuniões e noitadas, risos e desespero. Obrigado por seres um exemplo para mim como amiga e como profissional.

À Catarina, a minha parceira de Ciência e Oncologia desde o secundário, nem sonhávamos as voltas que a vida ia dar para 8 anos depois estarmos a trabalhar em laboratórios frente a frente. Como nem todas as voltas que a vida deu neste tempo foram boas, permite-me dedicar também um pouquinho desta dissertação ao teu pai. Obrigado por seres um exemplo de coragem e seres a prova viva de que quando metemos um sonho na cabeça não há nada nem ninguém que nos possa parar.

A todos os meus amigos online, particularmente ao Coelho, ao Luís e à Lúcia, por serem o meu momento de pausa do dia-a-dia. Obrigado por estarem sempre lá para me ouvir e para "palhaçar", porque nem tudo na vida tem que ser levado a sério.

À minha equipa de andebol de praia, os Full Stamina, por me permitirem voltar todos os anos ao desporto onde fiz casa e que me ajudou ao longo de toda a vida. Obrigado por todos os treinos e jogos onde a cabeça limpa de tudo o que se passa à minha volta.

A todos os meus restantes amigues, Sofia, Mariana, Kika, Catarina, Manu, Sara, Cisca e a todos aqueles que marcaram momentos felizes da minha vida nos últimos 6 anos, o meu mais sincero obrigado.

E, no final, os agradecimentos mais importantes. À minha família: a minha mãe, o meu pai, a minha irmã, o Brown, a minha tia e os meus avós. Apesar de não gostar de o expressar de maneira muito efusiva, quero que saibam que são a parte mais importante da minha vida. Sem o vosso apoio nada disto teria sido possível. Obrigado aos meus pais por me terem ensinado todos os valores fundamentais da vida, por me empurrarem para a frente quando a vontade me faltava e por me terem dado todas as condições que poderia pedir para ter sucesso na vida. Obrigado à minha irmã por me fazer sempre tentar ser uma pessoa melhor e o melhor exemplo possível para ela. Obrigado aos meus avós e à minha tia por todo o carinho que me dão e sempre me deram. Obrigado ao Brown, o meu animal de apoio emocional a quem só falta falar, eu sei que não vais ler isto, mas sei que quando te ler vais perceber tudo. Somos poucos, mas somos bons, e isso é tudo o que importa.

Por fim, e mais importante de tudo, um obrigado à pessoa que me fez seguir o caminho da Oncologia, o meu tio. Infelizmente já não cá estás neste momento importante para mim, mas espero que me estejas a ver do sítio onde estiveres com muito orgulho. O meu objetivo continua a ser o mesmo, dar o melhor de mim para que pelo menos uma pessoa não passe pelo que tu passaste. Acho que estou no bom caminho. Até já!

"I will try to imprint what I know in my soul. Carry it so deeply in the pockets of my existence, that when I open my eyes and look down at my new hands, I will already know. I will be ready. I will remember." – The Art of Racing in the Rain

RESUMO

Introdução: O cancro da tiroide é o cancro mais frequente do sistema endócrino e o 9º mais prevalente a nível mundial. As taxas de incidência têm vindo a aumentar nas últimas décadas, não apenas devido ao sobrediagnóstico, mas também em consequência de alterações nas exposições ambientais e do aumento concomitante de doenças metabólicas, como a diabetes mellitus.

O subtipo mais comum de cancro da tiroide, o carcinoma papilar da tiroide, responsável por 80 a 90% dos novos casos, apresenta na maioria das situações um excelente prognóstico. No entanto, 5 a 10% dos doentes desenvolvem doença metastática agressiva, o que requer investigação adicional sobre os mecanismos moleculares envolvidos. A patologia molecular subjacente ao carcinoma papilar da tiroide passa pela disfunção de vias de sinalização como as MAPK e PI3K/AKT/mTOR, associadas ao metabolismo energético celular.

Sendo que estas vias também estão implicadas em distúrbios metabólicos como a diabetes mellitus, surgiu o racional para explorar o potencial de fármacos antidiabéticos — nomeadamente a metformina (inibidor do complexo mitocondrial I) e a canagliflozina (inibidor do co-transportador de sódio-glucose tipo 2, SGLT2) — como possíveis estratégias terapêuticas no carcinoma da tiroide.

Métodos: O efeito dos medicamentos antidiabéticos metformina e canagliflozina em linhas celulares de carcinoma papilar da tiroide foi avaliado por microscopia eletrónica de transmissão, de modo a observar alterações morfológicas, particularmente mitocondriais. Foi também realizado um teste de stress glicolítico para aferir a capacidade de ambos os medicamentos induzirem alterações metabólicas nas células.

A expressão das proteínas GLUT1, GLUT3, GLUT4, SGLT2, MCT1 e MCT4 foi observada por imunofluorescência e quantificada por cromatografia líquida–espectrometria de massa (CL-EM).

Adicionalmente, procedeu-se à análise proteómica das linhas celulares BCPAP, TPC-1 e Nthy Ori 3-1.

Resultados: Os resultados de microscopia eletrónica de transmissão demonstram que a canagliflozina induziu um aumento significativo na área total mitocondrial na linha celular Nthy Ori 3-1, enquanto a metformina induziu um aumento significativo no número de gotas lipídicas na linha TPC-1. O teste de stress glicolítico demonstrou a capacidade da canagliflozina esgotar significativamente a reserva glicolítica nas células BCPAP, enquanto a metformina provocou diminuições significativas da reserva glicolítica como uma percentagem nas linhas BCPAP e Nthy Ori 3-1. Durante o tratamento, a glicólise também foi significativamente menor após a administração de metformina nas linhas celulares tumorais.

Todos os transportadores e co-transportadores em estudo foram observados por imunofluorescência; porém, o GLUT4 e o SGLT2 não foram detetados por western blot nem por CL-EM. Relativamente aos níveis de expressão da linha Nthy Ori 3-1, a linha

BCPAP apresenta níveis de expressão inferiores de GLUT3 e níveis superiores de MCT4, enquanto a linha TPC-1 exibe níveis mais baixos de GLUT1 e MCT4 e níveis mais elevados de MCT1.

A análise proteómica permitiu identificar proteínas diferencialmente expressas e vias enriquecidas do Gene Ontology e Reactome entre as três linhas celulares e entre as duas linhas tumorais e a linha Nthy Ori 3-1.

Conclusão: Tanto a metformina como a canagliflozina induziram uma alteração metabólica favorecendo a glicólise em linhas celulares de carcinoma papilar da tiroide. Os resultados deste estudo indiciam um potencial papel dos medicamentos antidiabéticos como terapia coadjuvante para o carcinoma papilar da tiroide.

Palavras-chave: Carcinoma Papilar da Tiroide; Metabolismo; Diabetes; Metformina; Canagliflozina

ABSTRACT

Background: Thyroid cancer (TC) is the most prevalent endocrine cancer and the 9th most prevalent cancer worldwide. The incidence rates have been increasing in the last decades, not only due to overdiagnosis but also as a result of changes in environmental exposures and the parallel increase in metabolic diseases, particularly diabetes mellitus.

The most common TC subtype, papillary thyroid cancer, responsible for 80 to 90% of new cases, presents an excellent prognosis in most cases. However, 5 to 10% of patients develop aggressive metastatic disease, requiring further investigation into the molecular mechanisms driving its progression. The underlying molecular pathology of PTC involves the dysfunction of signalling pathways, such as MAPK and PI3K/AKT/mTOR, related to cellular energy metabolism.

Given that these pathways are also implicated in metabolic disorders like diabetes mellitus, this rationale has prompted the exploration of anti-diabetic drugs—namely metformin (a mitochondrial complex I inhibitor) and canagliflozin (a sodium–glucose cotransporter 2 [SGLT2] inhibitor)—as potential therapeutic strategies for thyroid cancer.

Methods: The effect of anti-diabetic drugs metformin and canagliflozin on PTC cell lines was assessed by transmission electron microscopy (TEM) to evaluate morphological alterations, particularly mitochondrial changes. A glycolysis stress test was performed to examine the ability of both drugs to induce metabolic shifts.

Additionally, protein expression of GLUT1, GLUT3, GLUT4, SGLT2, MCT1 and MCT4 was analysed by immunofluorescence and quantified by liquid chromatography-mass spectrometry (LC-MS).

In addition, a comparative proteomic analysis was conducted on the BCPAP, TPC-1 and Nthy Ori 3-1 cell lines.

Results: TEM results showed that canagliflozin significantly increased the total mitochondrial area in Nthy Ori 3-1 cells, while metformin induced a significant increase in the number of lipid droplets in TPC-1 cells. The glycolysis stress test demonstrated that canagliflozin markedly depleted the glycolytic reserve of BCPAP cells, whereas metformin significantly reduced the glycolytic reserve as a percentage in both BCPAP and Nthy Ori 3-1 cells, and also lowered glycolysis during drug exposure in the two tumour cell lines.

All transporters and co-transporters under study were detected by immunofluorescence; however, GLUT4 and SGLT2 were not observed by western blot nor by LC-MS. Comparing with the expression levels of the Nthy Ori 3-1 cell line, the BCPAP cell line presents a lower expression level of GLUT3 and a higher level of MCT4, whilst the TPC-1 cell line presents downregulation of GLUT1 and MCT4 and upregulation of MCT1 expression.

Proteomics analysis successfully identified differentially expressed proteins and revealed enriched Gene Ontology and Reactome pathways both among the three cell lines and between the two cancer cell lines and the Nthy Ori 3-1 cell line.

Conclusions: Both metformin and canagliflozin induced metabolic alterations consistent with a shift towards glycolysis in papillary thyroid cancer cell lines. These findings suggest a potential role for anti-diabetic drugs as adjuvant therapeutic agents in papillary thyroid cancer.

Keywords: Papillary Thyroid Cancer; Metabolism; Diabetes; Metformin; Canagliflozin

TABLE OF CONTENTS

FIGURES INDEX

TABLES INDEX

LIST OF ABBREVIATIONS

A

AdipoR1 – adiponectin receptor 1

AdipoR2 – adiponectin receptor 2

AKT – AKT serine/threonine protein kinases

ALK – anaplastic lymphoma kinase 1

AMP – adenosine monophosphate

AMPK – AMP activated protein kinase

ANG - angiogenin

ARE – antioxidant response element

ATC – anaplastic thyroid carcinoma

ATP – adenosine triphosphate

B

B2M – beta-2-microglobin

Bax – BCL2-associated X protein

Bcl-2 – beta-cell lymphoma 2

BMI – body mass index

BRAF - B-RAF proto-oncogene, serine/threonine kinase

C

CA proteins – cancer associated proteins

cAMP – cyclic adenosine monophosphate

CCL2 - chemokine (C-C motif) ligand 2

CD70 – cluster of differentiation 70

CDK4 – cyclin-dependent kinase 4

CDKN2A – cyclin-dependent kinase inhibitor 2A

CHK2 – checkpoint kinase 2

c-JNK – c-Jun n-terminal kinase

CO_2 – carbon dioxide

COL1A1 – collagen type 1 alpha 1

COL5A1 – collagen type 5 alpha 1

D

DAPI - 4′,6-diamidino-2-phenylindole

DDR1 - discoidin domain receptor tyrosine kinase 1

DHGTC – differentiated high grade thyroid cancer

DMSO – dimethyl sulfoxide

DNA - deoxyribonucleic acid

DPP-4 - dipeptidyl peptidase-4

E

ECAR – extracellular acidification rate

EGFR – endothelial growth factor

ERK - extracellular signal-regulated kinases

F

FAIMS - Field Asymmetric Ion Mobility Spectrometry

FAK - focal adhesion kinase

FDR – false discovery rate

FNA – fine-needle aspiration

FT4 – serum free thyroxine

FTC – follicular thyroid carcinoma

G

GDH – glutamate dehydrogenase 1

GLP-1 – glucagon-like peptide 1

GLUT – glucose transporter

GLUT1 – glucose transporter 1

GLUT10 – glucose transporter 10

GLUT3 – glucose transporter 3

GLUT4 – glucose transporter 4

GO – Gene Ontology

GSK3β - glycogen synthase kinase-3 beta

H

HCC – hepatocellular carcinoma

HEMS – Histology and Electron Microscopy

HIF1α – hypoxia-inducible factor 1-alpha

HK2 – Hexokinase 2

HLA-A - major histocompatibility complex, Class I, A

HLA-B - major histocompatibility complex, Class I, B

HO-1 – heme oxygenase 1

HRAS – Harvey Ras

I

I3S – Instituto de Investigação e Inovação em Saúde

IARC – International Agency for Research in Cancer

IEFV-PTC – invasive encapsulated follicular variant of papillary thyroid carcinoma

IGF – insulin growth factor

IGF-1 – insulin growth factor 1

IGF-2 – insulin growth factor 2

IGFBP – insulin growth factor binding proteins

IGF-IR – insulin growth factor receptor 1

IGF-IIR – insulin growth factor receptor 2

IL-8 – interleukin 8

IPCS – International Programme on Chemical Safety

IR – insulin receptor

IR-A – insulin receptor A

IR-B – insulin receptor B

IRS-1 – insulin substrate 1

IRS-2 – insulin substrate 2

J

JNK – Jun n-terminal kinase

K

KRAS – Kirsten Ras

L

LC-MS – liquid chromatography-mass spectrometry

LDHA – lactate dehydrogenase A

LRP2 - low-density lipoprotein receptor-related protein 2

M

MAPK – mitogen-activated protein kinases

MASLD – metabolic dysfunction associated steatotic liver disease

MCT – monocarboxylate transporter

MCT1 – monocarboxylate transporter 1

MCT4 – monocarboxylate transporter 4

MET - hepatocyte growth factor receptor

MetS – metabolic syndrome

MGPDH - mitochondrial glycerophosphate dehydrogenase

MHC – major histocompatibility complex

MKI – multi-kinase inhibtors

mRNA – messenger ribonucleic acid

MTC – medullary thyroid carcinoma

mTOR – mechanistic target of rapamycin

N

NADPH - nicotinamide adenine dinucleotide phosphate

Nedd4 - neural precursor cell expressed developmentally down-regulated protein 4

NF-κB - nuclear factor kappa-light-chain-enhancer of activated B cells

ngRPMI – no-glucose RPMI medium

NOX4 - NADPH oxidase 4

NQO1 – NADPH quinone dehydrogenase 1

NRAS – neuroblastoma Ras

NRF2 – NFE2-related factor 2

NTRK - neurotrophic tyrosine receptor kinase

O

OB-R – leptin receptor

OCT1 – organic cation transporter 1

OIS – oncogene induced senescence

OSIS – oxidative stress induced senescence

OTC – oncocytic thyroid carcinoma

P

p70S6K - p70 ribosomal protein S6 kinase

PBS – phosphate-buffered saline

PBS-T – PBS-1% Tween20

PDGFR - platelet-derived growth factor receptor

PDTC – poorly differentiated thyroid carcinoma

PGC-1β - peroxisome proliferator-activated receptor gamma coactivator 1 beta

PI3K - phosphatidylinositol 3-kinase

PKA – protein kinase A

PKC – protein kinase C

PKM2 – pyruvate kinase muscle 2

PP2A – protein phosphatase 2A

PPBI - Portuguese Platform of Bioimaging

pS6 - phosphorylated S6 ribosomal protein

PTC – papillary thyroid carcinoma

pTERT – TERT promoter

PTPN2 - tyrosine-protein phosphatase non-receptor type 2

R

RAF - RAF proto-oncogene serine/threonine kinase

RAI-R – radioiodine refractory

RAS – RAS proto-oncogene family

RET – rearranged during transfection

RIPA – radioiodineprecipitation assay

RNEM – Portuguese Mass Spectrometry Network

ROS – reactive oxygen species

RPMI - Roswell Park Memorial Institute

RPMIc – complete RPMI medium

S

SAHF – senescence associated heterochromatin foci

SGLT – sodium-glucose co-transporter

SGLT1 - sodium-glucose co-transporter 1

SGLT2 - sodium-glucose co-transporter 2

SHC - Src Homology 2 Domain Containing Transforming Protein 1

SREBP1 - sterol regulatory element-binding protein 1

STAT3 - signal transducer and activator of transcription 3

T

T2DM – Diabetes mellitus type 2

TBS – Tris-buffered saline

TBS-T – TBS-1% Tween20

TC – thyroid cancer

TCA – tricarboxylic acid

TEM – transmission electron microscopy

TERT – telomerase reverse transcriptase

TIMP-1 - tissue inhibitors of metalloproteinase-1

TNF – tumour necrosis factor

TNF-α – tumour necrosis factor alpha

TOM - translocase of outer mitochondrial membrane

TOMM20 - translocase of outer mitochondrial membrane 20

TP53 – tumour protein 53

TSH – thyroid stimulating hormone

U

USP2 - ubiquitin-specific peptidase 2

V

VEGF – vascular endothelial growth factor

VEGF-A – vascular endothelial growth factor A

VEGFR – vascular endothelial growth factor receptor

W

WDTC – well-differentiated thyroid cancer

WHO – World Health Organization

Wnt - wingless-related integration site

γ

γ-H2AX - phosphorylated Histone H2AX

INTRODUCTION

Thyroid Cancer

Epidemiology

Thyroid cancer (TC) is the most common endocrine malignancy worldwide (1). According to Globocan data, in 2022, thyroid cancer is the 7th most prevalent cancer, with over 821,000 cases, whilst being the 24th in terms of mortality, causing an estimated 44,000 deaths. Because its incidence is three times higher in women, it ranks as the 5th most prevalent cancer for women (2).

The incidence of TC cases has been on the rise worldwide since the 1980s, especially in developed countries, despite the mortality figures being constant through time. This indicates a problem with overdiagnosis of the tumour, with over 75% of the cases reported by the World Health Organization (WHO) from 2013 up to 2017 being attributable to overdiagnosis (3). In the USA, the incidence of thyroid cancer has increased by 300% in 3 decades, with a median age of diagnosis of 51 years being considerably lower than most other cancer types, but an estimated 5-year survival of 98.1% reflecting the indolent nature of most thyroid neoplasms (4).

Risk Factors

Ionizing radiation exposure during childhood was up to this decade the only well-established modifiable risk factor for TC, but recent studies have suggested that other factors may also play a role (5). Benign thyroid diseases, such as benign nodules and goitre show an association with elevated TC risk, despite no causal relationship being established, whereas hypothyroidism and hyperthyroidism show weaker positive associations (6). Iodine deficiency or excess is also associated with TC risk, but further studies still need to be performed (5). Obesity and higher body mass index (BMI) have been linked with a higher risk of TC, as is the case for many other cancer types (7). The International Agency for Research on Cancer (IARC) has also considered excess adiposity to have a causal relationship with TC (8). The underlying mechanisms are not yet fully understood, although chronic inflammation and insulin resistance have been the most extensively studied (5). Birthweight is positively associated with higher TC risk for both the newborn and the mother, whereas cigarette smoking and alcohol consumption are inversely correlated to TC risk (5). Endocrine-disrupting chemicals, as defined by the WHO and the International Programme on Chemical Safety (IPCS), are 'exogenous substances or mixtures that alter the functions of the endocrine system and consequently cause adverse health effects in an intact organism, its progeny, or (sub-)populations.' (9), that include pesticides, flame retardants, polychlorinated biphenyls, phthalates, perfluoroalkyl substances and Bisphenol A, have also been associated with an increased risk of thyroid cancer, although the specific carcinogenic effects of each subclass remain unclear (10).

Subtypes

Well-differentiated thyroid cancer (WDTC), originating from follicular thyroid cell carcinogenesis, accounts for over 90% of all thyroid cancer cases and includes papillary thyroid carcinoma (PTC), follicular thyroid carcinoma (FTC), invasive encapsulated follicular variant of PTC (IEFV-PTC), oncocytic thyroid carcinoma (OTC), and differentiated high-grade thyroid carcinoma (DHGTC). On the other hand, medullary thyroid cancer (MTC), which arises from parafollicular C cells carcinogenesis, represents approximately 5% of thyroid cancer cases (11).

Diagnosis and Treatment

Diagnosis of thyroid cancer (TC) is typically initiated *via* thyroid palpation, followed by an ultrasound. If in the ultrasound images, the thyroid presents nodules with high-risk features, such as irregular margins, punctate echogenic foci and extrathyroidal extension, fine needle aspiration (FNA) is recommended (12). The FNA cytology results are reported utilizing the standardized Bethesda classification system, that allows the stratification and standardization of results into 6 categories, each with its own implied malignancy risk: (i) nondiagnostic; (ii) benign; (iii) atypia of undetermined significance; (iv) follicular neoplasm; (v) suspicious for malignancy; and (vi) malignant (13). Management options include active surveillance, recommended for small and low-risk PTCs; minimally invasive interventions, that include radiofrequency, microwave and laser ablations, recommended for intra-thyroidal PTCs of less than 10 mm; and the most common option for WDTCs, surgery, that can be either a lobectomy or a thyroidectomy. The postoperative management can include radioiodine therapy and thyrotropin suppression, to be evaluated on a case-by-case basis. Despite the good prognosis and the efficacy of the surgical treatment for most TC cases, 5 to 15% of patients that undergo radioiodine therapy develop radioiodine-refractory (RAI-R) disease, considerably worsening their prognosis (12). For these cases, systemic therapies have been approved, with multikinase inhibitors (MKIs) like lenvatinib and sorafenib being the first-line treatment for RAI-R WDTC, whilst cabozantinib acts as second-line treatment. Other targeted treatments such as the use of *RET* (Rearranged during transfection) inhibitors or NTRK (neurotrophic tyrosine receptor kinase) inhibitors can also be used in RAI-R DTC cases. Furthermore, immune checkpoint inhibitors are being studied and showing promising results (14).

Since overdiagnosis of TC is harmful due to unnecessary surgery, cost of treatment, psychological effects and severe decrease in quality of life, guidelines discourage screening in asymptomatic individuals (12). The global increase in the number of thyroid cancer cases has been driven by the overdiagnosis of small low-risk PTC due to use of thyroid ultrasounds, especially in developed countries. However, the increase in incidence-based mortality of patients with small tumours suggests a change in the biological profile of the tumours, confirming that overdiagnosis was not the sole factor behind the increase in TC incidence (4).

Papillary Thyroid Cancer

Epidemiology

Papillary thyroid carcinoma is the most common subtype of thyroid cancer and the one with the best prognosis, with long-term survival figures higher than 90%, despite a rather high recurrent disease appearance value of 25% to 35%.The clinical challenge for PTC treatment is to differentiate the aggressive tumours from the majority good prognosis tumours (11).

Genetic Profile

Several driver mutations have been linked to malignancy, but none have proven useful for guiding treatment or predicting clinical outcomes. In papillary thyroid carcinomas, the most common genetic alterations, occurring in a mutually exclusive manner in nearly 70% of cases, are *BRAF* (B-RAF proto-oncogene, serine/threonine kinase) mutations, particularly *BRAF V600E*, and *RAS* (*RAS* proto-oncogene family) point mutations. *RET* fusion are the most common non-mutation gene alterations. These genetic alterations constitutively active the MAPK (mitogen-activated protein kinases) and/or PI3K (phosphatidylinositol 3-kinase) signalling pathways (11). Despite not being driver mutations, *TERT* (telomerase reverse transcriptase) promoter (p*TERT*) mutations are associated with aggressiveness, especially when coexisting with *BRAF* mutations (15). Since PTC presents a low somatic mutation burden and the driver mutations are mutually exclusive, the differences between *BRAF V600E*-like PTC and *RAS*-like PTC have been well-established (16).

BRAF

BRAF is a serine/threonine protein kinase of the *RAF* (*RAF* proto-oncogene serine/threonine kinase) family and has been shown to be mutated and constitutively activated in 7% of all cancers. *BRAF* point mutations lead to constitutive activation of the MAPK pathway, leading to cell differentiation, proliferation, growth, and apoptosis (11). *BRAF V600E* is the most prevalent point mutation in PTC, being identified in 29% to 69% of cases, and has been associated with recurrence and lymph node metastasis. However, the value of *BRAF* mutations has prognostic markers is still undetermined, as clinico-pathological features and concomitant genetic alterations play a key role in the development of the disease (17).

TERT

TERT encodes the telomerase reverse transcriptase and two hotspot mutations have been identified in the promoter region of the gene (C228T and C250T). p*TERT* mutations promote telomerase activity and preserve telomere's length (11). These mutations, despite being present in only 11.3% to 12.3% of cases, show a more established

relationship with aggressive features, such as metastasis, and are the most reliable molecular marker to predict persistence/recurrence and disease-specific mortality. In particular, the coexistence of *BRAF V600E* and p*TERT* mutations have been associated with PTC specific mortality, although the synergetic mechanisms of the mutations remain unclear (17).

RAS

RAS, comprised of *HRAS* (Harvey Ras), *KRAS* (Kirsten Ras), and *NRAS* (neuroblastoma Ras), are a family of GTP (guanosine triphosphate) binding proteins that play a key role in controlling cell growth, differentiation, and survival through the MAPK (where it acts upstream compared to *BRAF*) and PI3K-AKT (AKT serine/threonine protein kinases) signalling pathways. It is constitutively activated due to mutations in codons 12, 13 and 16 and the mutations are present in benign lesions, FTC and PTC, limiting its value in then prediction of clinical outcomes (11).

RET

RET encodes a tyrosine-kinase receptor responsible for activating downstream cascades, such as the MAPK signalling pathway. *RET* has multiple fusion partners in PTC, with the most common being *RET/PTC1* and *RET/PTC3*, the latter especially common in post-Chernobyl children. These rearrangements, whose prevalence varies deeply across studies (2.5% to 73%), are responsible for maintaining the tyrosine-kinase domain intact and constitutively activating the MAPK signalling pathway (11).

Multi-Omics Profile

A multi-omics study of papillary thyroid carcinoma published in 2024 revealed that the molecular differences between PTC and normal thyroid tissue extend beyond the genetic level to the protein and metabolite levels. The study identified pronounced metabolic alterations in PTC, including upregulation of valine, leucine, and isoleucine degradation; arginine and proline metabolism; pyruvate metabolism; and both glycolysis and gluconeogenesis pathways. Necroptosis and apoptosis were also identified as significantly enriched pathways. Using the glycolysis pathway as an example, it is important to note that whilst some enzymes were downregulated at the mRNA level, some others were upregulated at the protein and phospho-protein levels, revealing the importance of crossing data from multiple omics approaches (18).

Metabolism Regulation in TC

Otto Warburg proved in the 1920s that cancer cells opted for glycolysis over oxidative phosphorylation even in aerobic conditions, a phenomenon now known as the Warburg effect (19). Thyroid cancer is no exception to this rule and its metabolic reprograming affects not only glucose metabolism, but also lipid, amino acid and nucleotide metabolisms. Alterations to glucose metabolism are the most well-studied, with TC cells showing a preference for glycolysis over oxidative phosphorylation. This behaviour leads to an increased production of NADPH (nicotinamide adenine dinucleotide phosphate) and other biomass synthesis due to the shift of glycolytic intermediaries to the pentose phosphate pathway, which makes nucleotides more accessible and facilitates cell proliferation. Due to the conversion of pyruvate into lactate, the latter exerts effects in the transcription activity of the cell through participation in histone modifications. The higher emissions of CO_2 (carbon dioxide) and lactate also acidify the tumour microenvironment, affecting immune response. The metabolic shift in TC needs to be supported through an higher glucose uptake rate (20).

The transport of glucose through the cell membrane occurs through glucose transporters (GLUTs) or sodium-glucose co-transporters (SGLTs). Glucose transporters 1, 3, 4 and 10 (GLUT1, GLUT3, GLUT4 and GLUT10) are the glucose transporters present in all thyroid cells. In thyroid cancer, GLUT1 is the only transporter consistently overexpressed across all tumour types, indicating its central role in increased glucose uptake. GLUT1 and GLUT3 are both hypoxia-inducible and contribute to PTC progression. GLUT expression is negatively associated with tumour differentiation, with anaplastic thyroid cancers showing higher GLUT1 levels than well-differentiated thyroid cancers. In PTC, GLUT1, GLUT3, and GLUT4 are present, although GLUT1 is the least expressed among them (21).

Lactate transport is mediated by monocarboxylate transporters, such as monocarboxylate transporter 1 (MCT1), a bidirectional lactate transporter, and monocarboxylate transporter 4 (MCT4), responsible for lactate efflux. Within the cell, it is transported to the mitochondria *via* the translocase of the outer mitochondrial membrane (TOM complex). In PTC, MCT1 is poorly expressed, which contrasts with its high expression in ATC (anaplastic thyroid cancer), suggesting a potential role of the transporter in TC aggressiveness. MCT4 is upregulated in cancer associated fibroblasts and in stromal cells of PTC, suggesting high levels of efflux of lactate, promoting acidification to the tumour microenvironment. TOMM20 (translocase of outer mitochondrial membrane 20) is upregulated in PTC cells (22).

In PTC, the *BRAF V600E* mutation induces the overexpression of lactate dehydrogenase (LDHA), a key enzyme for glycolysis, whose high levels have been associated with worse response to treatment and prognosis (23). Furthermore, *BRAF V600E* also inhibits mitochondrial metabolism through the overexpression of HIF1α (hypoxia-inducible factor 1-alpha) that leads to the inhibition of PGC-1β (peroxisome proliferator-activated receptor gamma coactivator 1 beta), an activator of oxidative phosphorylation-related mitochondrial genes (24).

Metabolic Diseases

Epidemiology

Metabolic diseases, characterized by chronic metabolic disfunctions, encompass numerous diseases such as Diabetes mellitus types 1 and 2, obesity, hypertension, hypercholesterolemia and metabolic dysfunction associated steatotic liver disease (MASLD). This group of diseases pose a significant burden on the lifes of patients increasing the risk of cardiovascular disease and stroke, for example, and often coexist in the same patient. From 1990 to 2021, whilst the burden of hypertension and hypercholesterolemia decreased worldwide, the burden of diabetes mellitus type 2 (T2DM) and obesity has increased at a rate of 0.42 % per year and 0.26 % per year, respectively (25). This can be explained due to the fact that the prevalence of these diseases has been rising considerably over the past decades, with 60% of the population in European countries suffering from obesity and 9% of the population in Western countries suffering from diabetes, of which 90% are T2DM (26).

Obesity

Obesity has been linked with an increased risk of TC. A meta-analysis published in 2024 revealed a significant and positive correlation between adiposity indicators and the risk of thyroid cancer (27). In the United States, 13.6% of the total increase in PTC prevalence from 1995 to 2015 has been attributed to the simultaneous rise in the incidence of overweight and obese populations, with the figures jumping to 57.8% when considering only large PTC cases (tumours with more than 4 cm). It is estimated that in 2015, for adults older than 60 years, one in six PTCs and two in three large PTCs may have been attributable to overweight and obesity (28). Curiously, studies demonstrate that obesity is more strongly associated with *BRAF*-mutated PTC than with non *BRAF*-mutated PTC cases, although the underlying mechanisms for this association remain unclear (29).

Although the mechanisms linking obesity to thyroid cancer are not yet fully understood, several pathways have been proposed, including elevated cytokine levels and oxidative stress from chronic systemic inflammation, dysregulation of adipokines (increased leptin and decreased adiponectin), and the development of insulin resistance accompanied by elevated insulin-like growth factor 1 (IGF-1) (30).

Metabolic Syndrome

Metabolic syndrome (MetS), also known as insulin-resistance syndrome, is not a disease in of itself, but rather a pathological state characterized by central obesity, insulin resistance, hypertension and hyperlipidaemia by the WHO in 2022. MetS is diagnosed when 3 of the 5 following criteria are met: hyperglycaemia, arterial hypertension, hypertriglyceridemia, low high-density lipoprotein cholesterol and increased waist circumference. It has been linked with more than 50 different types of cancer, including thyroid cancer (31). In Portugal, in 2015, 33.4% of the population between 25 and 74

years of age suffered from metabolic syndrome, a value slightly higher than the world estimated prevalence of around 25%, representing a major health issue that affects a high proportion of the population (32). Mechanisms such as insulin resistance, adipokine dysregulation and chronic inflammation are observed in MetS patients, further underlining its correlation with other metabolic diseases such as obesity and diabetes and replicating them as a severe risk factor for cardiovascular disease and stroke (33). A meta-analysis published in 2018 found that insulin-resistance, dysglycaemia, high BMI and hypertension increased the risk for thyroid cancer. However, MetS was not associated with risk of TC (34).

Diabetes Mellitus

Diabetes mellitus is a metabolic disorder classified by two different types: type 1 diabetes mellitus is characterized by a deficiency in insulin secretion by pancreatic β-islet cells and type II diabetes mellitus (T2DM) is characterized by insulin-resistance. Both types cause dysregulation of glucose homeostasis due to alterations on the insulin levels. Diabetes is associated with multiple co-morbidities such as nephropathy, retinopathy, neuropathy, atherosclerosis, heart disease and cardiovascular dysfunction. Diabetes has also been associated with a higher risk for several cancer types, such as breast, gastric, colorectal, and pancreatic cancers (35). In fact, diabetes patients have a worse prognosis after chemotherapy or surgery and a higher mortality rate than non-diabetic patients with the same cancer types. However, the molecular mechanisms of cancer in diabetic patients have not yet been fully understood. Both diseases share some common features, including elevated insulin and insulin-like growth factor 1 (IGF-1) levels, dysregulated leptin/adiponectin secretion, and immune abnormalities. Furthermore, cancer cells undergo a metabolic shift that increases their glucose demand, depriving neighbouring cells of essential energy and inducing a state of cachexia, a condition responsible for around 20% of all cancer-related deaths and which can be exacerbated by diabetes. This impaired metabolic homeostasis also leads to production of reactive oxygen species (ROS), that in its turn leads to the accumulation of DNA damage that can trigger carcinogenesis. On the other hand, DNA repair systems require a lot of energy, inducing mitochondrial stress and dysfunction, commonly observed in diabetes-induced cancer (36).

For thyroid cancer, many studies have shown a relation between diabetes and higher TC risk: a prospective cohort study by Aschebrook-Kilfoy et al (37); a retrospective cohort study by Linkeviciute-Ulinskiene et al (38); a meta-analysis by Yeo et al (39); a case-control study by Zhan et al (40); a systematic review and meta-analysis by Yin et al (34); a case-control study by Seo et al (41); a population-based cohort study by Carstensen et al (42); a meta-analysis of cohort studies by Li et al (43); a meta-analysis of cohort studies by Dong et al (44); a cross-sectional analysis by Saewai et al (45); and a prospective study in two USA cohorts by Hu et al (46). Some non-hereditary mechanisms have been proposed to link diabetes with the higher risk of TC (35).

Linking Mechanisms of Diabetes and Thyroid Cancer

Secretion of Thyroid Stimulating Hormone

Thyroid stimulating hormone (TSH), also known as thyrotropin, is a thyroid growth factor that plays a fundamental role in the proliferation of TC cells. It regulates the growth and proliferation of thyroid cells by binding to the TSH receptors, activating adenylate cyclase and increasing the levels of cAMP (cyclic adenosine monophosphate) and PKA (protein kinase A) (35). A high level of TSH accompanied by normal serum free thyroxine (FT4) is characteristic of subclinical hypothyroidism, which has been associated with poor glycaemic control in T2DM patients (47). Furthermore, high levels of TSH have been associated with a higher risk factor for PTC (48). In fact, TSH suppression is used as post-operative treatment for patients that undergo lobectomy or thyroidectomy procedures (12). In PTC, high TSH levels disrupt the p53-induced senescence mechanism in *BRAF V600E*-mutated thyroid cancer cells, promoting tumour progression (49). In PDTC (poorly differentiated thyroid cancer), high levels of TSH regulate angiogenesis and proliferation through the activation of the AKT and ERK (extracellular signal-regulated kinases) pathways and subsequent upregulation of VEGF-A (vascular endothelial growth factor A) and IL8 (interleukin 8) (50). In summary, it is of the upmost importance to control the TSH serum levels of patients, especially those affected by T2DM.

Oxidative Stress

Oxidative stress occurs when the levels of reactive oxygen species (ROS) and other free radicals reach extremely high levels, either due to excessive production or deficient degradation (35). PTC patients present higher levels of oxidative stress, significant oxidative DNA damage and a damaged antioxidant system (51). Oxidative stress induces the upregulation of PTPN2 (tyrosine-protein phosphatase non-receptor type 2), a regulator of tyrosine kinase signalling, in thyroid cancer cells, promoting the progression of thyroid cancer (52). In addition, Nrf2 (NFE2-related factor 2), an antioxidant transcription factor, is upregulated in PTC, maintaining redox homeostasis *via* the activation of HO-1 (heme oxygenase 1) and NQO1 (NADPH quinone dehydrogenase 1), between others, promoting proliferation *via* the Nrf2/ARE/NQO1 (ARE, antioxidant response element) signalling pathway (53). Oxidative stress is linked with insulin-resistance and T2DM through multiple pathways. Free radicals can damage the plasma membrane, serving as an important signal for the activation of IRS-1 (insulin receptor substrate 1), which in turn activates the PI3K pathway. When insulin levels exceed the optimal concentration, PI3K shifts from its normal function to enhance the activity of NOX4 (NADPH oxidase 4), an oxidizing enzyme that generates additional ROS. Plasma membrane damage induced by ROS can also impair the function of glucose transporters and, more broadly, disrupt phosphorylation processes, thereby interfering with normal insulin signalling. Furthermore, oxidative stress may trigger retromer activation *via* CK2 (casein kinase 2), signalling for GLUT4 (glucose transporter 4) degradation, leading to hyperglycaemia. ROS also act in the periphery of the membrane by impairing insulin

receptor signal transduction, causing insulin resistance. Compensatory hyperinsulinemia, the production of excessive insulin to compensate the reduction of glucose uptake, can also desensitize peripheral tissues to insulin, further aggravating insulin resistance. At the mitochondrial level, in pancreatic beta cells, oxidative stress can contribute to mitochondrial malfunction, limiting energy production, causing beta cell death by apoptosis, and amplifying stress signals, that can lead to insulin resistance and diabetes. Furthermore, excess ROS can activate transcription factors, for example, NF-κB (nuclear factor kappa-light-chain-enhancer of activated B cells), an immune and inflammatory response mediator that promotes an insulin-resistant environment by activating PKC (protein kinase C) (54). This evidence shows the common role of oxidative stress in both tumour and T2DM disease progression.

Hyperinsulinemia and Insulin-Like Growth Factor-1

IGF-1 (insulin-like growth factor 1) is ligand of the IGF (insulin growth factor) system, that binds to IGF-IR (IGF receptor I), a tyrosine kinase receptor, modulating multiple biological processes. The system is mediated by IGFBPs (IGF binding proteins) and is complemented by IGF-2 (insulin-like growth factor 2) and IGF-IIR (IGF receptor II). It interacts with insulin and insulin receptors A (IR-A) and B (IR-B). IGF-IR expression levels are upregulated in WDTC, suggesting a potential mitogenic effect of IGF-1. When activated, IGF-IR activates multiple downstream signalling pathways, such as the RAS/RAF/ERK (RAF, RAF proto-oncogene serine/threonine-protein kinase) pathway *via* SHC (Src Homology 2 Domain Containing Transforming Protein 1), the PI3K/AKT/mTOR (mTOR, mechanistic target of rapamycin) pathway *via* IRS-1 (insulin receptor substrate 1) and the FAK (focal adhesion kinase) pathway *via* IRS-2 (insulin receptor substrate 2). These pathways are responsible for increased cell growth and motility, protein synthesis, cell cycle progression and negative regulation of apoptosis. The crosstalk between TSH and the IGF system is also important. TSH stimulates cAMP activity, which promotes the Nedd4 (neural precursor cell expressed developmentally down-regulated protein 4) dependent ubiquitination of IRS-2, enhancing IGF-dependent mitogenic signalling. There is also crosstalk between the IGF system and several tyrosine-kinase receptors: insulin receptors (IR), epidermal growth factor receptor (EGFR), vascular endothelial growth factor receptor (VEGFR), platelet-derived growth factor receptor (PDGFR), hepatocyte growth factor receptor (MET), the discoidin domain receptor tyrosine kinase 1 (DDR1) and the anaplastic lymphoma kinase 1 (ALK), to name a few. Because these receptors share common downstream pathways, dysregulation of any single pathway can indirectly affect the IGF system (55). Consequently, hyperinsulinemia and elevated IGF-1 levels may contribute to thyroid carcinogenesis in diabetic patients.

Secretion of Adipocytokines

White adipose tissue is the most abundant type of adipose tissue in humans, responsible for storing excess energy as triglycerides and playing a central role in energy regulation, including glucose homeostasis and insulin sensitivity. In addition, it functions as an

endocrine organ by releasing adipocytokines such as leptin, adiponectin, and resistin (56).

Leptin regulates appetite, with higher levels supressing it, and modulates metabolism through the food intake-fasting energy peaks and lows. Although it is known that insulin promotes the secretion of leptin, its association with diabetes is still a controversial topic and more studies need to be performed (56). The leptin receptor (OB-R) is overexpressed in papillary thyroid cancer cells, and leptin induces cell proliferation *via* the PI3K/AKT signalling pathway, suggesting a potential association with TC (57).

Adiponectin is an adipocytokine that modulates insulin levels, exerting an anti-diabetic effect. Higher adiponectin levels are associated with lower T2DM risk and, at the same time, significantly lower adiponectin serum levels are observed in T2DM patients (56). Lower levels of circulating adiponectin have been observed in thyroid cancer patients. Furthermore, PTC cells show lower levels of adiponectin receptors, AdipoR1 and AdipoR2, and this sub-expression of the receptors is linked with extrathyroidal invasion, polycentricity, and higher TNM stages. Activation of the Adiponectin receptors leads to the inhibition of PI3K/AKT, ERK1, Wnt/GSK3β/β-catenin (wingless-related integration site / glycogen synthase kinase-3 beta / β-catenin), STAT3 (signal transducer and activator of transcription 3), USP2 (ubiquitin-specific peptidase 2), and Bcl-2 (B-cell lymphoma 2) signals and to the activation of AMPK (AMP-activated protein kinase), c-JNK (c-Jun N-terminal kinase) and Bax (BCL2-associated X protein) signals, regulating cell survival, growth and proliferation, cell cycle arrest and apoptosis (58). Adiponectin can also counteract the tumorigenic effects of leptin in cell proliferation, migration and invasion (59).

Resistin is an adipocytokine that counteracts insulin and is mainly expressed in the abdominal adipose tissue, connecting obesity with diabetes and validating the waist-hip ratio as a risk measurement for T2DM (56). Higher serum resistin levels are observed in TC patients and have been proposed has a risk factor for lymph node metastasis (60).

Secretion of Inflammatory Factors and Chemokines

T2DM patients commonly suffer from chronic hyperglycaemia that leads to chronic inflammation, promoting the secretion of cytokines and chemokines (35). Higher levels of serum inflammatory factors, such as the neutrophil/lymphocyte ratio, the platelet/lymphocyte ratio and the levels of C-reactive protein and IL-27 have been found in WDTC patients (61), whilst higher levels of IL-6 and CXCL8, were found in thyroid cancer tissues. This is promoted by endoplasmatic reticulum stress (ER-stress) caused by hypoxia and nutrient deprivation and leads to dedifferentiation of TC cells and weakens their radioiodine uptake capacity (62). TNF-α (tumour necrosis factor alpha), an inflammatory factor that has the capacity to promote the production of granulocyte-colony stimulating factor, stimulate vasoactive mediators and induce the expression of VEGF (vascular endothelial growth factor), has also been associated with TC (63).

Anti-Diabetic Drugs

With the relationship between diabetes and thyroid cancer well established, studies have investigated the potential effects of anti-diabetic drugs on thyroid cancer. Several classes of drugs are used to treat T2DM, including biguanides, sulfonylureas, glinides, thiazolidinediones, DPP-4 (dipeptidyl peptidase-4) inhibitors, SGLT2 (sodium-glucose co-transporter 2) inhibitors, GLP-1 (glucagon-like peptide-1) analogues, and insulin analogues. Among these, some have demonstrated potential anti-tumour effects in thyroid cancer, notably biguanides (e.g., metformin), SGLT2 inhibitors (e.g., canagliflozin), DPP-4 inhibitors and thiazolidinediones. The repurposing of anti-diabetic drugs for cancer treatment is hugely beneficial in several ways, being more cost- and time-effective than the production of new drugs, since these drugs have already surpassed safety, pharmacology, and toxicology tests to be approved for clinical use (64).

Metformin

Metformin is one of the most used anti-diabetic drugs in the treatment of T2DM and was first synthesized in 1920. It exerts its action by inhibiting the mitochondrial complex I, a key member of the electron transport chain, leading to the inhibition of oxidative phosphorylation and reducing the production of ATP (adenosine triphosphate). This mechanism also activates AMPK, a protein kinase responsible for the regulation of glucose metabolism, lipid metabolism and energy homeostasis, through the increased levels of cellular AMP (adenosine monophosphate). In fact, the effects of metformin affect such a vast number of cellular mechanisms that not all of them are fully understood at this point. However, studies suggest that metformin treatment may have beneficial effects not only in diabetic patients but also in a range of conditions, including cancer, neurodegenerative, liver, renal, and cardiovascular diseases (65).

A meta-analysis has detected a 0.68-fold decrease in TC risk in patients undergoing metformin treatment, with a particular reduction in incidence observed in Eastern countries, such as China and South Korea (66).

Metformin has been shown to directly impact TC through both direct and indirect mechanisms. Studies with TC cell lines and animal models have demonstrated the potential effects of metformin as a pro-apoptotic drug (67). Metformin inhibited cell cycle progression, induced apoptosis, antagonized the growth-stimulatory effect of insulin, inhibited clonal cell growth and reduced thyroid cancer sphere formation (68). Metformin induced apoptosis through AMPK activation in PTC cell lines and restricted tumour growth and volume, whilst AMPK levels increased and AKT and mTOR levels decreased, in an *in vivo* xenograft mouse model (69). In WDTC cell lines, metformin inhibited cell growth through activation of AMPK and down-regulation of p70S6K/pS6 (p70 ribosomal protein S6 kinase / phosphorylated S6 ribosomal protein) (70). Metformin induced ER-stress and ER stress-associated apoptosis in TPC-1 cells, a PTC cell line, and in an *in vivo* xenograft mouse model (71). In another study with the TPC-1 cell line, metformin supressed proliferation and induced apoptosis through the downregulation of LRP2 (low-density

lipoprotein receptor-related protein 2) and inhibition of the JNK (Jun N-terminal kinase) pathway (72).

Other potential mechanisms through which metformin may act on thyroid cancer have also been investigated, particularly regarding cell metabolism. Thakur et al demonstrated that OCT1 (organic cation transporter 1), the metformin intracellular transporter, and MGPDH (mitochondrial glycerophosphate dehydrogenase), a respiratory chain dehydrogenase that links glycolysis and oxidative phosphorylation, are overexpressed in TC tissue. Furthermore, the study shows that metformin inhibited the increased cell proliferation and shift to oxidative phosphorylation promoted by MGPDH levels, rather inducing inhibition of cell growth and mitochondrial respiration, shifting towards glycolysis. Metformin effect was proportional to the expression levels of MGPDH in PTC cell lines and a xenograft mouse model (73). Another study demonstrated a metformin-induced inhibition of glucose uptake and mitochondrial respiration accompanied by a metabolic shift to glycolysis with a decrease of glycolytic reserve in PTC cell lines (74). Metformin also induced the downregulation of GLUT1 (glucose transporter 1), responsible for glucose uptake in the cell, and HK2 (hexokinase 2), a key enzyme in the glycolysis pathway, in PTC cell lines and a xenograft mouse model (75). Bikas et al found that metformin inhibited the expression of PKM2 (pyruvate kinase muscle 2), a glycolytic gene that was upregulated in thyroid cancer cells, and demonstrated that the shift in PKM2 isoforms was sufficient to provoke the metabolic shift to aerobic glycolysis. The same study also found that the pro-apoptotic and metabolic regulator roles of metformin in TC are also verified in low-glucose levels, similar to those observed in non-diabetic individuals, underlining that metformin may help the entire population and not only those already suffering from diabetes (76).

In 2023, the first study on the transcriptomics and metabolomics of the effects of metformin in TC was published. Using this multi-omics approach, it was demonstrated that metformin suppresses tumour cell proliferation and metastasis, promotes G1 phase cell cycle arrest, induces alterations in metabolic pathways involved in nucleotide, amino acid, and lipid synthesis, modulates DNA replication-related genes, regulates intermediate metabolites of the TCA (tricarboxylic acid) cycle and glutathione metabolism, and inhibits glycolysis (77). This study revealed the potential of multi-omics approaches in the understanding of the full extent of the effects of metformin in TC.

Importantly, metformin's anti-tumour effects were still observed *in vitro* when in a low-dose prolonged exposure setting, mimicking the treatment taken by diabetic patients in TC cell lines (78).

Canagliflozin

Canagliflozin is part of the SGLT2 inhibitors class of anti-diabetic drugs, one of the most recent new treatment approaches for diabetes, having only been approved in 2013. Canagliflozin inhibits both SGLT1 and SGLT2 (sodium-glucose co-transporters 1 and 2), but it presents a 400-fold higher affinity for the latter. SGLT2 is mainly present in the proximal tubule of the kidneys, where it is responsible for reabsorption of glucose from

urine to the bloodstream, but it is also present in pancreatic α-cells and in the cerebellum. Treatment with SGLT2 inhibitors as also been found to present cardiovascular and renal protection benefits (79).

In cancer, SGLT2 inhibitors have been found to possess anti-tumour effects in liver, pancreatic, prostate, bowel, lung and breast cancer, despite the full extent of the mechanism of action remaining unclear. In fact, SGLT2-independent effects have been described, such as AMPK activation, which leads to: induction of ferroptosis through inhibition of sterol regulatory element-binding protein 1 (SREBP1), a transcription factor regulating lipid biosynthesis, in breast cancer and hepatocellular carcinoma (HCC); induction of G2/M phase cell cycle arrest in HCC; and suppression of proliferation, G1 phase cell cycle arrest, and apoptosis induction *via* mTOR inhibition, in breast and pancreatic cancers. In HCC, mechanisms include inhibition of the glucose-induced translocation of β-catenin from the cytoplasm to the nucleus, resulting in inactivation of the Wnt/β-catenin signalling pathway, a metabolic pathway that promotes aerobic glycolysis. Canagliflozin also directly inhibits PP2A (protein phosphatase 2A), the responsible for the phosphorylation of β-catenin, leading to its proteasomal degradation. Canagliflozin also inhibited IL-8, ANG (angiogenin) and TIMP-1 (tissue inhibitors of metalloproteinase-1), pro-angiogenic proteins. Another mechanism of action of canagliflozin, observed in breast cancer cells, involves inhibition of cell proliferation through suppression of GDH (glutamate dehydrogenase), a key enzyme of the TCA cycle responsible for converting glutamate into α-ketoglutarate (80).

For thyroid cancer, very few data exist up to this point. A study published in 2022 reported increased SGLT2 expression in thyroid cancer tissue. Furthermore, experiments in PTC cell lines and in a xenograft mouse model demonstrated that canagliflozin inhibited cell growth and induced apoptosis *via* AMPK activation and subsequent inhibition of the AKT/mTOR signalling pathway. The study also demonstrates that canagliflozin affects glycolysis due to the limitation of glucose uptake and induced cell cycle arrest in G1 phase through the downregulation of cyclin D1, cyclin D3, cyclin E1, cyclin E2 and E2F1 expression levels. Lastly, canagliflozin stimulated the DNA damage response signalling ATM/CHK2 (CHK2, checkpoint kinase 2) activation through the upregulation of γ-H2AX (phosphorylated Histone H2AX), a marker of DNA damage (81). A more recent study showed that canagliflozin was able to reduce the secretion of pro-tumorigenic chemokines IL-8 and CCL2 (Chemokine (C-C motif) ligand 2) as well as inhibit the cell migration induced by the same chemokines, suggesting a potential tumour microenvironment regulatory role of canagliflozin (82).

Thus, it is crucial to investigate whether anti-diabetic drugs, particularly metformin and canagliflozin, modulate the metabolic profile of PTC. To address this, the present dissertation was designed with specific aims focused on assessing their effects on cellular metabolism, glucose and lactate transport, and global proteomic changes.

AIMS

Aims

The concomitant rise in cancer and metabolic disease incidence has put a spotlight on the research of the link between both malignancies. In the case of thyroid cancer, clinical data points to a relationship between diabetes mellitus and TC incidence and although several mechanisms have been suggested, the full extent of the relationship is still unknown. Furthermore, potential effects in TC prevention and therapy of the drugs used for diabetes treatment have been suggested, but there is still key information missing regarding their potential clinical applicability.

Having this in mind, the aim of this master's dissertation is to elucidate the effects of metformin and canagliflozin, two anti-diabetic drugs, on the metabolism of papillary thyroid cancer. With the main aim set, the project has been divided in 3 sections:

1. To evaluate the impact of metformin and canagliflozin on the metabolic activity of papillary thyroid cancer cell lines.
2. To characterize glucose and lactate transport in papillary thyroid cancer cell lines.
3. To define the proteomic profile of papillary thyroid cancer cell lines and assess alterations in protein expression and pathway enrichment.

MATERIALS AND METHODS

Cell Culture

Two papillary thyroid carcinoma cell lines – BCPAP and TPC-1 - and an immortalized human thyroid follicular epithelium cell line – Nthy Ori 3-1 – cell line (Table 1) were cultured in T75 flasks (TPP Techno Plastic Products AG, Trasadingen, Switzerland) in RPMI (Roswell Park Memorial Institute)-1640 medium (Capricorn scientific, Ebsdorfergrund, Germany), supplemented with 10% heat-inactivated Fetal Bovine Serum (Gibco, ThermoFisher Scientific, Waltham, Massachusetts, USA) and 1% Penicillin/Streptomycin (Gibco, ThermoFisher Scientific) (hereafter, RPMI complete medium or RPMIc). Cell cultures were grown at 37ºC with 5% CO_2 humidified environment in an incubator (HERACell 150i, ThermoFisher Scientific).

Table 1. **Characteristics of the thyroid cell lines used (83, 84).** *TP53*, Tumour Protein P53. WT, wildtype. -, not present. +, present.

Cell Line	Cell Type	*BRAF*	p*TERT*	*TP53*	*RET/PTC1*
BCPAP	Papillary thyroid carcinoma	V600E	C124T; C125T	D259Y	-
TPC-1	Papillary thyroid carcinoma	WT	C124T	WT	+
Nthy Ori 3-1	Immortalized human thyroid follicular epithelium	WT	WT	WT	-

Cell Treatment

Metformin (Stemcell™ Technologies, Canada) was prepared as a 1 mM stock solution in sterile 1× PBS (phosphate-buffered saline), whereas canagliflozin (MedChemExpress®, USA) was dissolved in DMSO (dimethyl sulfoxide) to obtain a 50 μM stock solution. Stock solutions were stored at −20°C according to the manufacturers' instructions. Working solutions for all treatments were freshly prepared by diluting the stock solutions in complete culture medium. Two types of controls were included in all experiments: for metformin, cells were treated with complete culture medium alone, and for canagliflozin, the control consisted of 0.1% DMSO in complete culture medium. DMSO is used as a solvent for canagliflozin treatment due to canagliflozin being insoluble in water. A study found that concentrations of 0.1% DMSO induced significant alteration in human cell lines, so a control group to assess the effects of canagliflozin had to be established (85). Treatment effects were assessed by comparing cells exposed to metformin or canagliflozin with their corresponding controls.

Transmission Electron Microscopy

Cells were plated in a 6-well plate with the following concentrations: 70,000 cells/mL for BCPAP, 20,000 cells/mL for TPC-1 and 60,000 cells/mL for Nthy Ori 3-1. The cells were incubated at 37ºC with 5% CO_2 in RPMIc medium for 24 hours. The next day, medium was removed, and cells were treated with either RPMIc, 20 mM metformin RPMIc, 0.1% DMSO RPMIc and 20 µM canagliflozin 0.1% DMSO RPMIc, according to their group and in triplicate wells. The cells were incubated at 37ºC with 5% CO_2 in the treated medium for 48 hours. Afterwards, cells were collected and centrifuged at 1,500 rpm for 5 minutes. The supernatant was discarded and the cells were handed to the Histology and Electron Microscopy facility at I3S.

For ultrastructural analysis, cells were fixed overnight at 4°C in a solution containing 2% formaldehyde and 2.5% glutaraldehyde in 0.1 M sodium cacodylate buffer. The cells were then washed with 0.1 M sodium cacodylate buffer, embedded in Histogel™, and post-fixed for 1 hour in 2% osmium tetroxide in 0.1 M sodium cacodylate buffer. Afterward, the cells were stained for 30 minutes with aqueous 1% uranyl acetate, dehydrated, and embedded in Embed-812 resin. Ultra-thin sections (70 nm thick) were cut using an RMC Ultramicrotome with Diatome diamond knives, mounted on 200 mesh copper grids, and stained with uranyless and 3% lead citrate for 5 minutes each. Imaging was done using a JEOL JEM 1400 transmission electron microscope, and digital images were captured with a PHURONA CCD camera.

Transmission electron microscopy was performed at the HEMS core facility at i3S, University of Porto, Portugal with assistance of Sofia Pacheco e Rui Fernandes. Images were analysed with QuPath 0.5.1 software.

The author acknowledges the support of the i3S Scientific Platform HEMS, member of the national infrastructure PPBI - Portuguese Platform of Bioimaging (PPBI-POCI-01-0145-FEDER-022122).

Immunofluorescence

Cells were plated in a 96-well plate with the following concentrations: 50,000 cells/mL for BCPAP, 20,000 cells/mL for TPC-1 and 40,000 cells/mL for Nthy Ori 3-1. The cells were incubated at 37ºC with 5% CO_2 in RPMIc medium for 24 hours. The next day, medium was discarded, and wells were washed with PBS and CellMask Deep Red Plasma Membrane stain (C10046, Invitrogen) 1:1,000 solution was added to the wells. After incubation at 37ºC with 5% CO_2 for 10 minutes,the staining solution was removed and cells were fixed with 4% paraformaldehyde for 30 minutes at room temperature. The cells were then treated with 0.1% Triton X-100 (Amresco LLC, Solon, OH, USA) for 15 minutes at room temperature. Triton X-100 was removed, and cells were washed with PBS-1% Tween-20 (hereafter, PBS-T) before blocking with 1% bovine serum albumin solution for 60 minutes at room temperature. Wells were incubated with primary antibody (Table 2) overnight at 4 ºC with agitation. The next day, cells were washed with PBS-T and incubated with a PhenoVue Hoechst 33342 (1:100,000) (Perkin Elmer ILC, Springfield,

IL, USA) and Alexa Fluor™ 488 Goat anti-Rabbit IgG antibody (1:1,250) (ThermoFisher) solution for 45 minutes at room temperature with agitation. After the incubation, wells were washed with PBS. Images were acquired with the Operetta CLS (Revvity, Inc. Waltham, Massachusetts, United States) and analysed with the Harmony High-Content Imaging and Analysis Software (Revvity, Inc.).

Table 2. **Characteristics of the primary antibodies used in immunofluorescence (IF) and western blot (WB).**

Antibody	Manufacturer	Clonality	Molecular Weight	IF Dilution	WB Dilution	Secondary Antibody
GLUT1	Abcam (ab15309)	Polyclonal	55 kDa	1:40	1:250	Anti-rabbit
GLUT3	Abcam (ab15311)	Polyclonal	54 kDa	1:100	1:1000	Anti-rabbit
GLUT4	Abcam (ab33780)	Polyclonal	50 kDa	1:60	1:500	Anti-rabbit
SGLT2	Invitrogen (PA5-101893)	Polyclonal	70 kDa	1:200	1:500	Anti-rabbit
MCT1	Invitrogen (PA5-72957)	Polyclonal	40 kDa	1:200	1:1000	Anti-rabbit
MCT4	Santa Cruz Biotechnology (sc-50329)	Polyclonal	43 kDa	1:100	1:2000	Anti-rabbit
αTubulin	Merck (T5168)	Monoclonal	55 kDa	Not used	1:5000	Anti-mouse

Protein Extraction and Quantification

Total protein was extracted from the three thyroid cell lines. Cells were collected and lysed *via* incubation with RIPA (Radioimmunoprecipitation Assay) buffer (50 mM Tris-HCl pH = 7.4, 150 mM NaCl, 2 mM EDTA, 1% NP-40, 0.1% SDS) supplemented with phosphatase and protease inhibitors for 15 minutes. Afterwards, samples were centrifuged at 14,000 rpm at 4ºC for 10 minutes and the supernatant was collected to a different Eppendorf tube, whilst the pellet was discarded.

Protein quantification was performed using the Bradford assay (Bio-Rad, Hercules, CA, USA) in a 96-well plate according to manufacturer's instructions. Absorbance was read at 650 nm on a SpectraMax® iD3 machine (Molecular Devices, San Jose, CA, USA).

Western Blot

Whole protein lysate (15 µg) was mixed with loading buffer (5 µL) and denatured at 95ºC for 5 minutes with agitation. Samples and Precision Plus Protein Standard Dual Color protein marker (Bio-Rad) were loaded in a 7.5% polyacrylamide gel and sodium dodecyl sulphate-polyacrylamide gel electrophoresis was ran at 100 V at room temperature for 45-90 minutes depending on the protein in analysis. Wet transfer was performed in a nitrocellulose membrane (Amersham, GE Healthcare, Chicago, IL, USA) at 500 mA at 4ºC for 2 hours. Membranes were washed with TBS (Tris-buffered saline)-1% Tween-20 (hereafter, TBS-T) and blocking was performed in 5% non-fat milk TBS-T for 1 hour at room temperature. Membranes were incubated with primary antibody (Table 2) overnight at 4 ºC with agitation. The next day, membranes were washed with TBS-T and incubated with the respective secondary antibody - IRDye® 800CW Donkey Anti-Rabbit antibody (1:20000) (LI-COR Biotech, Lincoln, NE, USA) or IRDye® 680CW Goat Anti-Mouse antibody (1:10000) (LI-COR Biotech) – at room temperature for 1 hour with agitation. Membranes were washed with TBS-T and revealed in an Odyssey ® CLx Infrared Imaging System (LI-COR Biosciences, Cambridge, UK), with readings at 800nm and 680nm according to the absorbance peaks of the secondary antibodies. Protein quantification was performed with Image Studio™ Lite software version 5.2.5 (LI-COR Biosciences). αTubulin was used as the housekeeping protein for normalization.

Glycolysis Stress Test

Cells were plated in Seahorse XF24 V7 PS Cell Culture Microplates with the following concentrations: 25,000 cells/well for BCPAP, 10,000 cells/well for TPC-1 and 20,000 cells/mL for Nthy Ori 3-1. The cells were incubated at 37ºC with 5% CO_2 in RPMIc medium for 24 hours. The next day, the procedure was conducted according to manufacturer's instructions. The assay was run in the Seahorse XFe24 Analyzer (Agilent, Santa Clara, CA, USA) and cells were exposed to the drugs *via* acute injection in the following order: either non -glucose RPMI (ngRPMI), 20 mM metformin ngRPMI, 0.1% DMSO ngRPMI or 20 µM canagliflozin 0.1% DMSO ngRPMI, according to their group and in quintuplicate wells, for 2 hours; 10 mM glucose; 1.0 µM oligomycin; and 50 mM 2-deoxyglucose (2-DG). Three measurements were recorded before any injection and after glucose, oligomycin and 2-DG injection. After metformin/DMSO/canagliflozin injection, fifteen measurements were recorded. For normalization, crystal violet protocol was performed and absorbance was measured using the Synergy 2 (BioTek) plate reader.

Liquid Chromatography-Mass Spectrometry

Whole protein lysate (100 µg) was collected handed to the Proteomics facility at I3S.

Each sample was processed for proteomic analysis following the solid-phase-enhanced sample-preparation (SP3) protocol and enzymatically digested with trypsin/LysC as previously described (86).

Protein identification and quantitation was performed by nanoLC-MS/MS equipped with a Field Asymmetric Ion Mobility Spectrometry - FAIMS interface. This equipment is composed of a Vanquish Neo liquid chromatography system coupled to an Eclipse Tribrid Quadrupole, Orbitrap, Ion Trap mass spectrometer (Thermo Scientific, San Jose, CA). 250 nanograms of peptides of each sample were loaded onto a trapping cartridge (PepMap Neo C18, 300 µm x 5 mm i.d., 174500, Thermo Scientific, Bremen, Germany). Next, the trap column was switched in-line to an Aurora Frontier XT 60 cm, 75µm (AUR4-60075C18-XT) chromatographic separation column. A 116 min separation was achieved by mixing A: 0.1% FA and B: 100% ACN, 0.1% FA with the following gradient at a flow of 250 nL/min: 2 min (0% B to 4% B), 20 min (4% B to 12% B), 65 min (12% B to 28% B), 11 min (28% B to 45% B), 2 min (45% B to 85 % B) and 16 min at 99% B. Subsequently, the column was equilibrated with 0% B. Data acquisition was controlled by Xcalibur 4.7 and Tune 4.2.4321 software (Thermo Scientific, Bremen, Germany).

MS results were obtained following a Data Dependent Acquisition - DDA procedure. MS acquisition was performed with the Orbitrap detector at 120 000 resolution in positive mode, quadrupole isolation, scan range (*m/z*) 375-1500, RF Lens 30%, standard AGC target, maximum injection time was set to auto, 1 microscan, data type profile and without source fragmentation. FAIMS mode: standard resolution, total carrier gas flow: static 4L/min, FAIMS CV: -45, -60 and -75 (cycle time, 1 s). Internal Mass calibration: Run-Start Easy-IC. Filters: MIPS, monoisotopic peak determination: peptide, charge state: 2-7, dynamic exclusion 30s, intensity threshold, $5.0e^3$. MS/MS data acquisition parameters: quadrupole isolation window 1.8 (m/z), activation type: HCD (30% CE), detector: ion trap, IT scan rate: rapid, mass range: normal, scan range mode: auto, normalized AGC target 100%, maximum injection time: 35 ms, data type centroid.

The raw data was processed using the Proteome Discoverer 3.1.1.93 software (Thermo Scientific) and searched against the UniProt database for the *Homo sapiens* reviewed proteome (2024_01 with 20,418 entries). A common protein contaminant list from MaxQuant was also included in the analysis. The MSPepSearch and Sequest HT and the search engines were used to identify tryptic peptides. The ion mass tolerance was 10 ppm for precursor ions and 0.5 Da for fragment ions. The maximum allowed missing cleavage sites was set to two. Cysteine carbamidomethylation was defined as constant modification. Methionine oxidation, deamidation of glutamine and asparagine, peptide terminus glutamine to pyroglutamate, and protein N-terminus acetylation, Met-loss, and Met-loss+acetyl were defined as variable modifications. Peptide confidence was set to high. The processing node Percolator was enabled with the following settings: maximum delta Cn 0.05; target FDR (strict) was set to 0.01 and target FDR (relaxed) was set to 0.05, validation based on *q*-value. Protein label-free quantitation was performed with the

Minora feature detector node at the processing step. Precursor ions quantification was performed at the consensus step with the following parameters: inclusion of unique plus razor peptides, precursor abundance based on intensity, and normalization based on total peptide amount. For hypothesis testing, protein ratio calculation was pairwise ratio-based and a t-test (background based) hypothesis test was performed.

Liquid chromatography-mass spectrometry was performed at the Proteomics core facility at i3S, University of Porto, Portugal with assistance of Hugo Osório.

A protein was considered enriched in a cell line if it met the following criteria: it was identified as a master protein, contained two or more unique peptide sequences, was detected in all three biological replicates of the enriched cell line with a high confidence score and exhibited a $\log_2$ fold change ≥ 1 in the expression comparison between cell lines.

Gene Ontology and Reactome pathways enrichment was analysed with the Panther classification system from the Gene Ontology knowledgebase website (87-89). For a pathway to be considered enriched in a cell line it had to have a false discovery rate (FDR) and a p value below 0.05.

The authors acknowledge the support of the i3S Scientific Platform Proteomics, integrated at RNEM, the Portuguese Mass Spectrometry Network.

Statistical Analysis

Statistical analysis was performed with GraphPad Prism Software version 8.0.1 (GraphPad Software, CA, USA). Non-parametric Mann Whiteny U test was performed for two-group comparisons.

RESULTS

Transmission Electron Microscopy

Transmission electron microscopy (TEM) was performed on BCPAP, TPC-1, and Nthy Ori 3-1 cell lines, both with and without treatment with metformin or canagliflozin for 48 hours. TEM images were analysed to assess several metabolic parameters, including the number of mitochondria, total mitochondrial area per cell, average area per mitochondrion, number of endosomes, and number of lipid droplets. Figure 1 presents representative images of the Control group for each cell line.

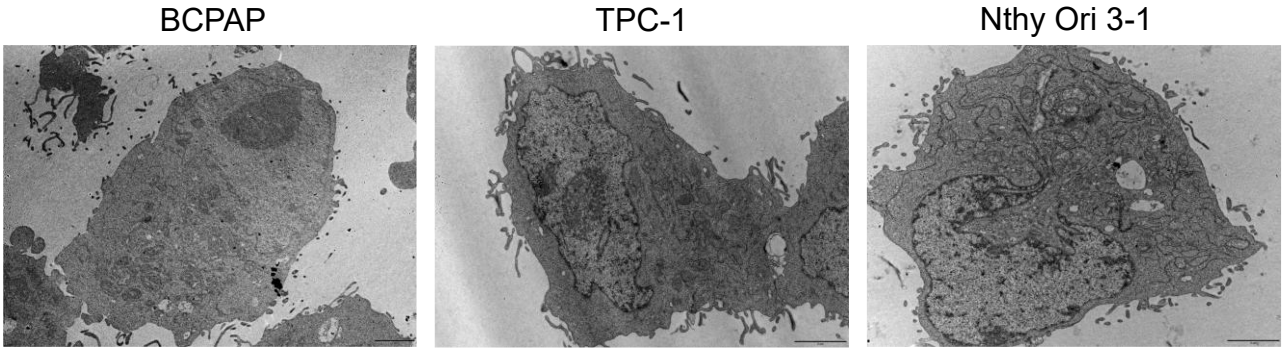

***Figure 1* – Representative Transmission Electron Microscopy Images.** Images of Control group. Scale bar, 2 µm.

The results shown in Figure 2 indicate an increase in the number of mitochondria following metformin treatment in TPC-1 cells, and after canagliflozin treatment in TPC-1 and Nthy Ori 3-1 cells. Metformin also induced an increase in the area per mitochondria in BCPAP and Nthy Ori 3-1 cells, whereas canagliflozin caused a decrease in mitochondrial area in Nthy Ori 3-1 cells. When expressed as a percentage of total mitochondrial area, these changes demonstrate an increase after metformin treatment in BCPAP cells and after canagliflozin treatment in TPC-1 cells. In Nthy Ori 3-1 cells, both drugs increased total mitochondrial area, with only the increase induced by canagliflozin reaching statistical significance.

Metformin increased the number of endosomes in TPC-1 and Nthy Ori 3-1 cells. Notably, DMSO treatment also led to an increase in endosome number across all cell lines, with a significant effect observed in Nthy Ori 3-1 cells. Regarding lipid droplets, metformin treatment increased their number from fewer than 1 to more than 3 per cell in both tumour cell lines, with a significant increase in TPC-1 cells. A slight increase was observed in Nthy Ori 3-1 cells, from nearly 0 to approximately 1 lipid droplet per cell.

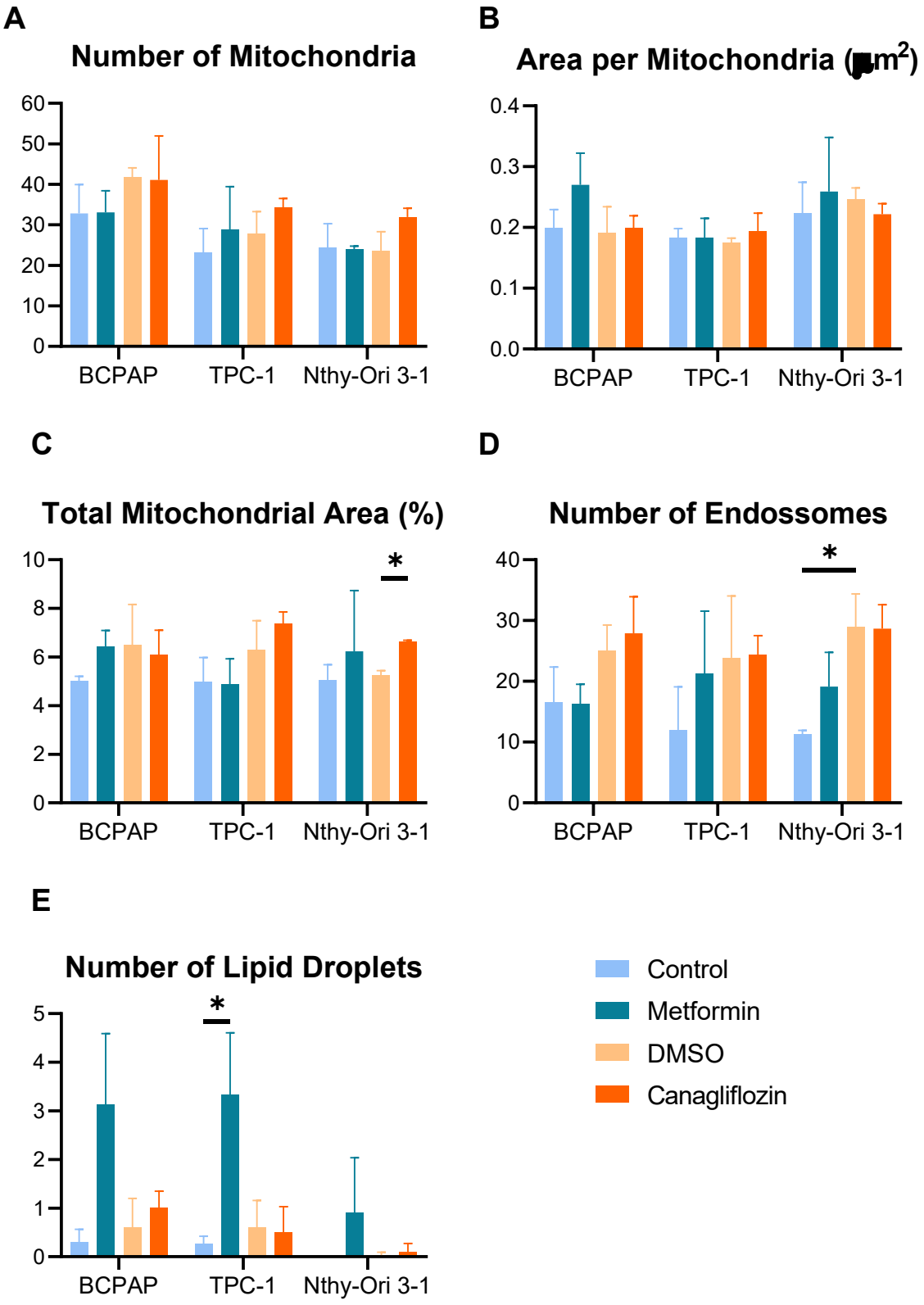

***Figure 2* – Transmission electron microscopy imaging analysis results (n=3).** Graph A, number of mitochondria per cell. Graph B, area per mitochondria (μm^2). Graph C, ratio of mitochondrial area per cell area. Graph D, number of endosomes per cell. Graph E, number of lipid droplets per cell. Control – no treatment; Metformin – 20 mM for 48 hours; DMSO – 0.1% for 48 hours; Canagliflozin – 20 μM for 48 hours. All images were analysed with QuPath v0.5.1 and statistical analysis was performed with GraphPad Prism Software version 8.0.1 (*, $p<0.05$).

Glycolysis Stress Test

Seahorse XF Glycolysis Stress Test was performed in the BCPAP, TPC-1 and Nthy Ori 3-1 cell lines with and without treatment with metformin or canagliflozin. The Seahorse XF instrument measures the extracellular acidification rate (ECAR) and uses the fact that glycolysis acidifies the medium to measure it. During the assay, cells were sequentially exposed to: glucose, to stimulate glycolysis; oligomycin, an ATP synthase inhibitor that shifts metabolism toward glycolysis by blocking mitochondrial ATP production; and 2-deoxyglucose (2-DG), a glucose analogue that inhibits glycolysis by binding to hexokinase (Figure 3). This approach allows the quantification of several parameters:

- Glycolysis: difference between the last measurement before glucose injection and the maximum measurement before oligomycin injection.
- Glycolytic capacity: difference between the last measurement before glucose injection and the maximum measurement after oligomycin injection.
- Glycolytic reserve: the difference between glycolytic capacity and glycolysis.
- Glycolytic reserve (%): the ratio of glycolytic capacity to glycolysis.
- Non-glycolytic acidification: the last rate measurement before glucose injection.
- Acute response: the difference between the last measurement before metformin, canagliflozin, or DMSO injection and the last measurement before glucose injection.

The results of the assay are presented in Figures 4 and 5.

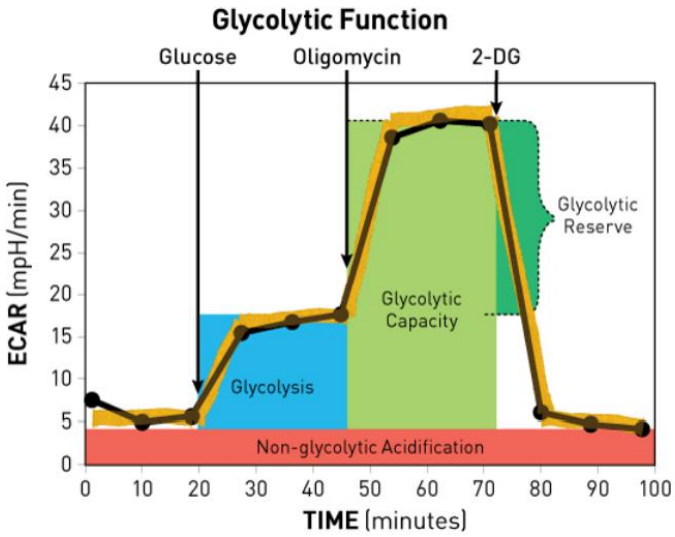

***Figure 3* – Seahorse XF Schematic of Glycolysis Stress Test.** Figure extracted from the manufacturer's user guide.

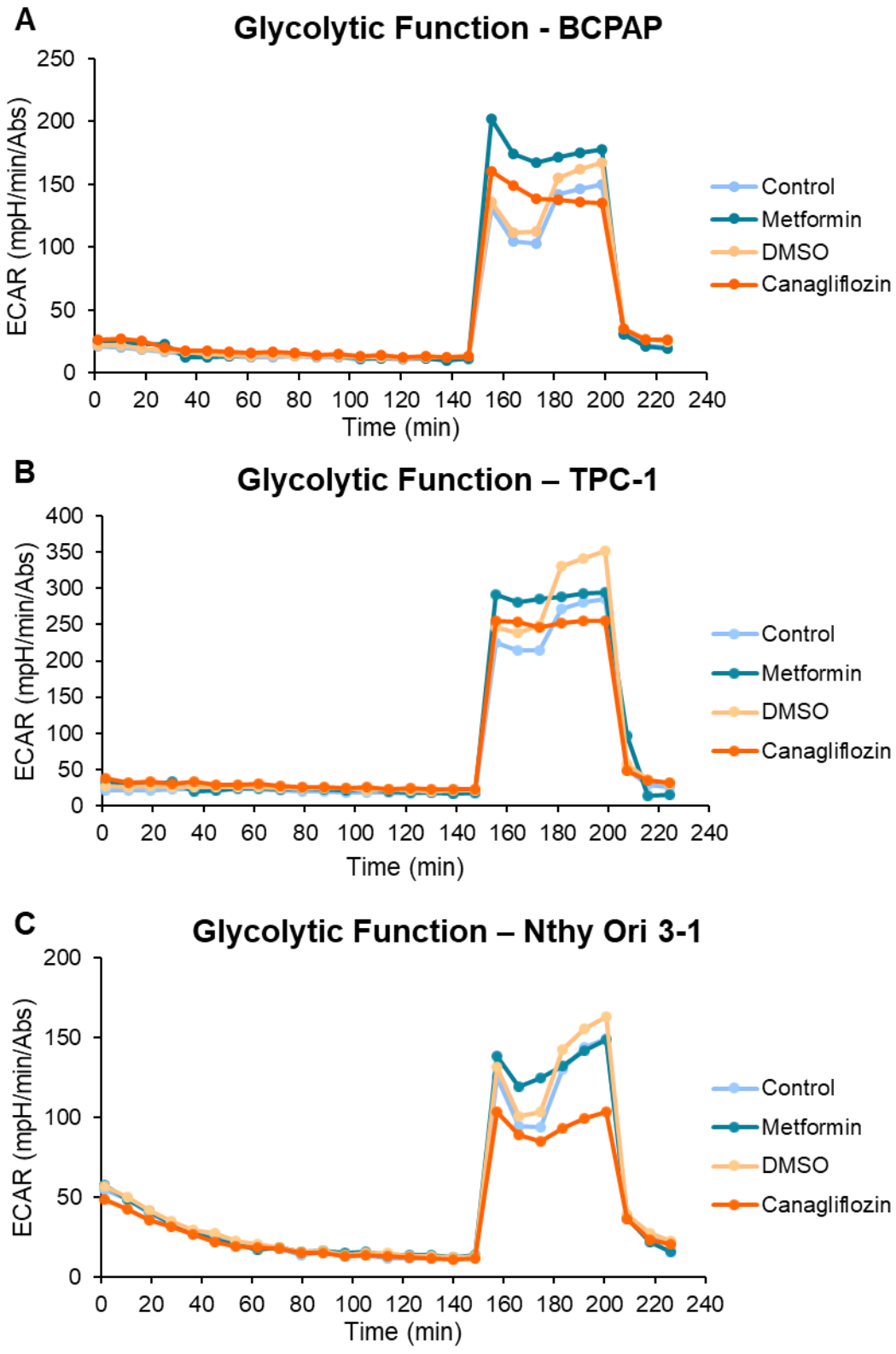

***Figure 4* - Glycolysis stress test.** Graph A, BCPAP glycolysis stress test. Graph B, TPC-1 glycolysis stress test. Graph C, Nthy Ori 3-1 glycolysis stress test. Control – no treatment, Metformin – 20 mM for 2 hours, DMSO – 0.1% for 2 hours, Canagliflozin – 20 μM for 2 hours. ECAR, Extracellular acidification rate.

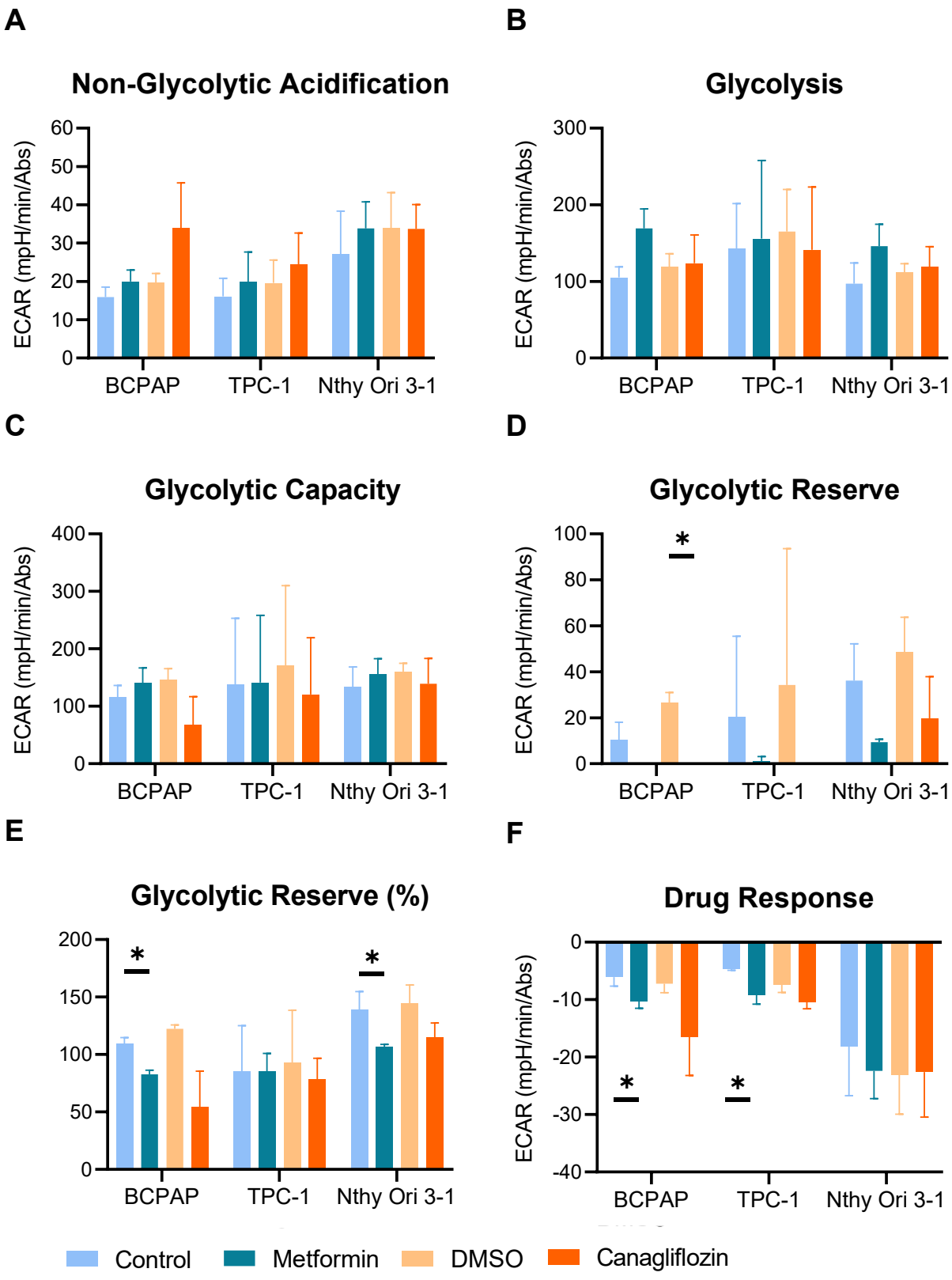

***Figure 5* – Glycolysis stress test analysis results (n=3).** Graph A, non-glycolytic acidification. Graph B, glycolysis. Graph C, glycolytic capacity. Graph D, glycolytic reserve. Graph E, glycolytic reserve as a percentage. Graph F, drug response. Control – no treatment; Metformin – 20 mM for 2 hours; DMSO – 0.1% for 2 hours; Canagliflozin – 20 µM for 2 hours. All images were analysed with QuPath v0.5.1 and statistical analysis was performed with GraphPad Prism Software version 8.0.1 (*, $p<0.05$).

Analysis of the data in Figure 5 shows that non-glycolytic acidification and glycolytic capacity were not significantly affected by treatment. Glycolysis was increased by metformin, particularly in BCPAP and Nthy Ori 3-1 cells. While all cell lines exhibited glycolytic reserves in the control and DMSO groups, only Nthy Ori 3-1 cells maintained reserves following treatment with the anti-diabetic drugs, whereas BCPAP cells showed a significant reduction in glycolytic reserve after canagliflozin treatment.

In percentage terms, TPC-1 cells displayed glycolysis exceeding their glycolytic capacity in all conditions, while Nthy Ori 3-1 cells never reached their glycolytic limit, despite a significant decrease in its glycolytic reserve after metformin treatment. BCPAP cells exceeded their reserve limit following treatment with both drugs, with metformin causing a significant reduction in the glycolytic reserve as a percentage.

Regarding drug effects prior to glucose injection, glycolysis was significantly reduced by metformin in both tumour cell lines and also decreased after canagliflozin treatment. Nthy Ori 3-1 cells did not show a significant response to either treatment, although they exhibited the largest reduction in inhibition among all conditions.

Immunofluorescence

Immunofluorescence assay was performed in the BCPAP, TPC-1 and Nthy Ori 3-1 cell lines to detect the expression of glucose transporters GLUT1, GLUT3 and GLUT4, sodium-glucose co-transporter SGLT2 and monocarboxylate transporters MCT1 and MCT4. DAPI (4′,6-diamidino-2-phenylindole) staining was used to mark cell nuclei.

The images presented in Figure 6 show the expression of all the proteins in study in all cell lines.

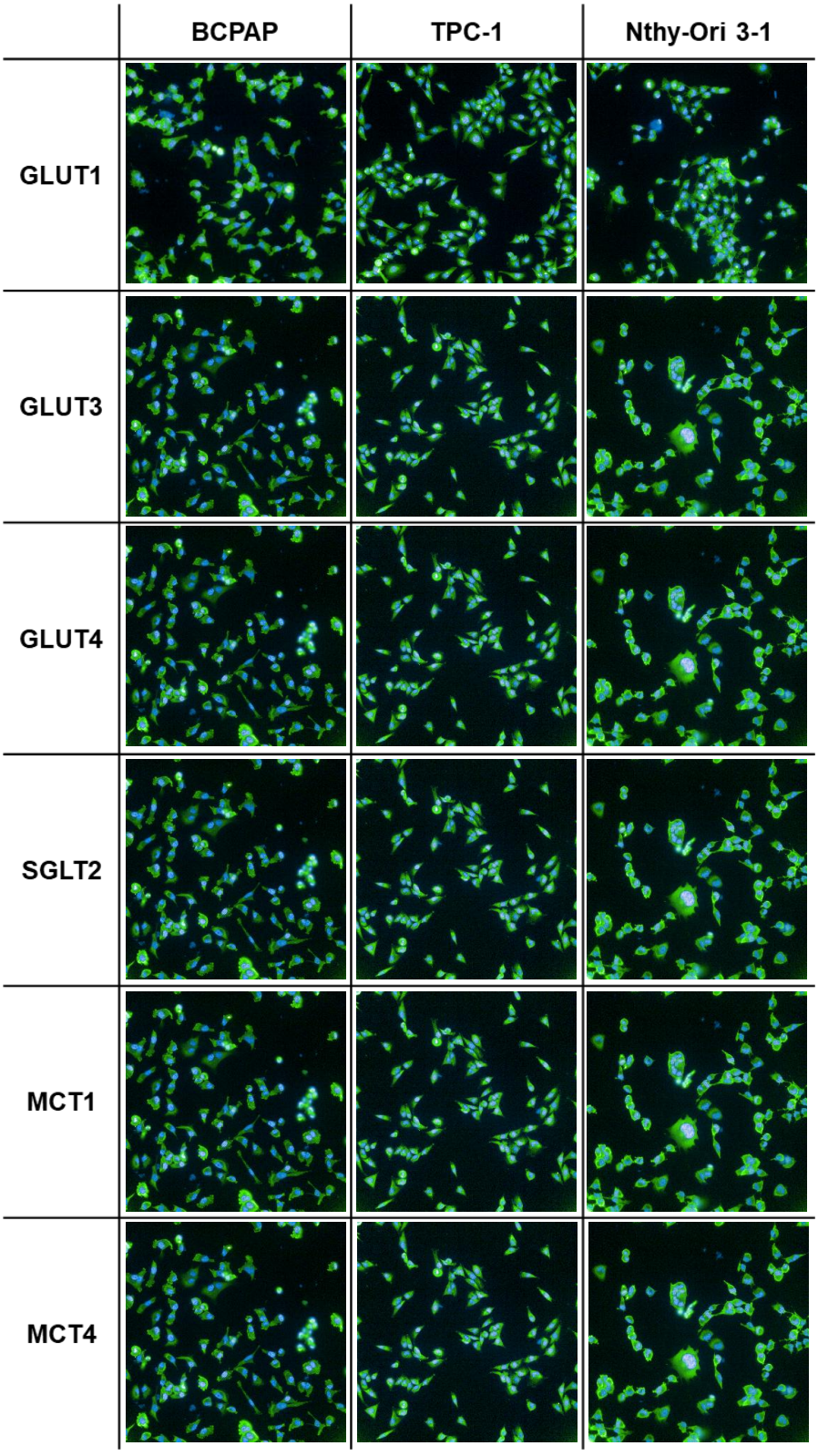

***Figure 6* – Representative immunofluorescence images.** From left to right: BCPAP, TPC-1 and Nthy Ori 3-1. From top to bottom: GLUT1, GLUT3, GLUT4, SGLT2, MCT1, MCT4. Merged channels: DAPI (blue), Alexa Fluor 488 Secondary Antibody (green).

Western Blot

Western blot assay was performed in the BCPAP, TPC-1 and Nthy Ori 3-1 cell lines for the relative quantification of the expression of glucose transporters GLUT1, GLUT3 and GLUT4, sodium-glucose co-transporter SGLT2 and monocarboxylate transporters MCT1 and MCT4. αTubulin was used as a house-keeping protein to normalize the expression levels of the transporters in study.

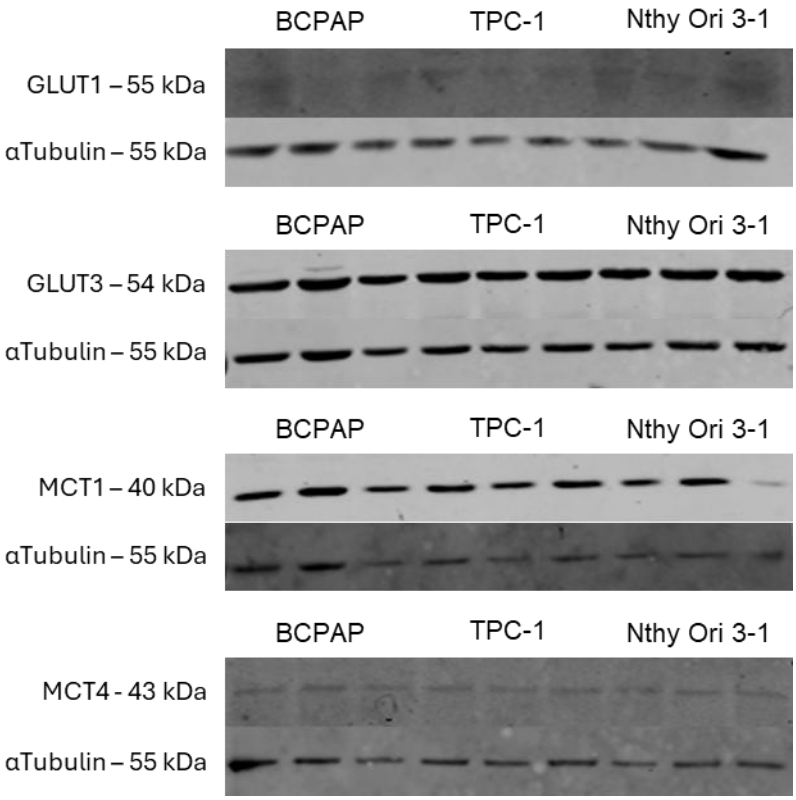

***Figure 7* – Western Blot membrane images.** From top to bottom: GLUT1, GLUT3, MCT1, MCT4. Membranes revealed with Odyssey ® CLx Infrared Imaging System at 680 nm for αtubulin detection and 800 nm for all other proteins.

GLUT4 and SGLT2 were not detected in any of the cell lines by Western blot analysis (Supplementary Data - Figure 1). The relative quantification shown in Figure 8 is normalized to protein expression in the Nthy Ori 3-1 cell line. Both GLUTs, and particularly both MCTs, were expressed at lower levels in BCPAP cells compared to Nthy Ori 3-1 cells. TPC-1 cells also exhibited reduced MCT1 and MCT4 expression—lower than in BCPAP cells—while maintaining similar levels of GLUT3 and higher levels of GLUT1 compared to the non-tumoural cell line.

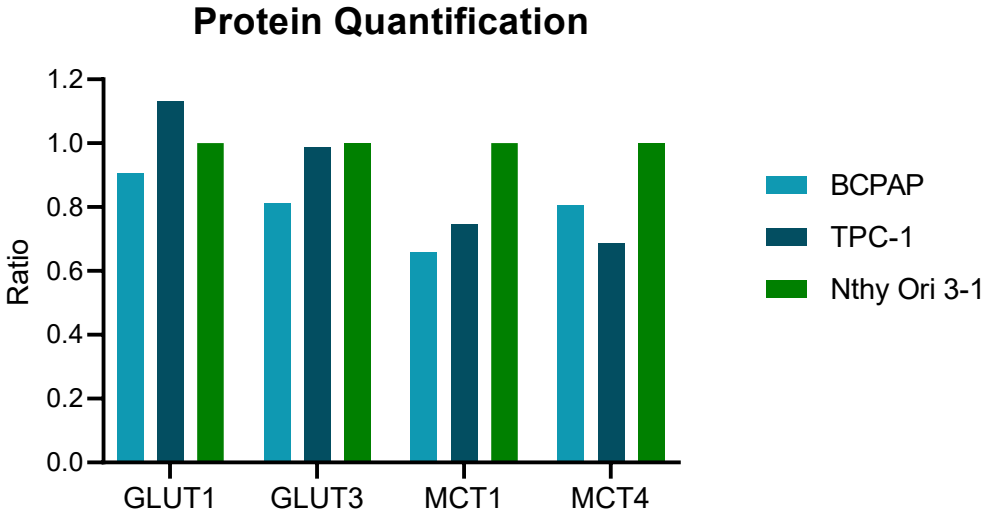

***Figure 8* – Relative protein quantification graph.** Values were normalized using αtubulin as a house-keeping gene. Values presented as ratio to Nthy Ori 3-1 expression. Membranes were analysed with Image Studio™ Lite software version 5.2.5.

Liquid Chromatography-Mass Spectrometry

Liquid chromatography-mass spectrometry was performed in the BCPAP, TPC-1 and Nthy Ori 3-1 cell lines for the absolute quantification of the expression of glucose transporters GLUT1, GLUT3 and GLUT4, sodium-glucose co-transporter SGLT2 and monocarboxylate transporters MCT1 and MCT4.

The heatmap and PCA plot (Figure 9) demonstrates the difference in protein expression between all cell lines.

Consistent with the Western blot results, GLUT4 and SGLT2 were not detected. Absolute protein quantification for GLUT1, GLUT3, MCT1, and MCT4 is presented in Figure 10. With the exception of GLUT3 in TPC-1 cells, all transporters were quantified with high confidence, and all observed differences were statistically significant. TPC-1 cells exhibited lower expression of GLUT1 and MCT4, but higher expression of MCT1 compared to the other two cell lines. GLUT1 and MCT1 levels were similar between BCPAP and Nthy Ori 3-1 cells. However, BCPAP cells expressed more MCT4, whereas Nthy Ori 3-1 cells showed higher GLUT3 expression.

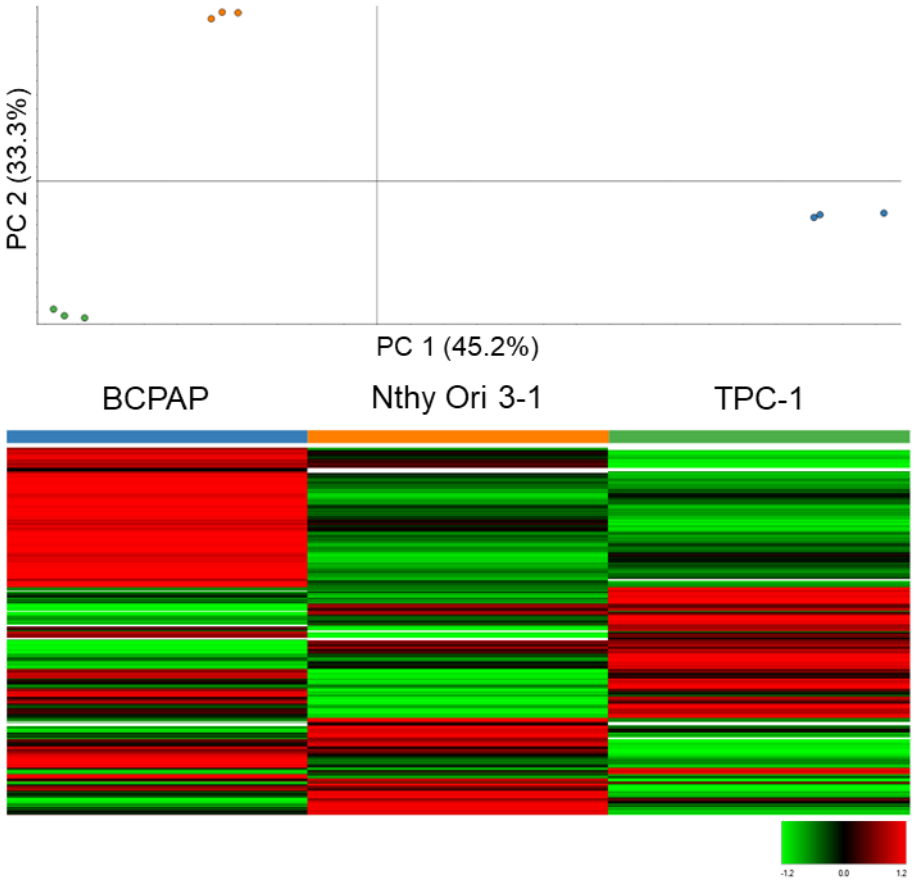

***Figure 9* - PCA plot and heat map of the proteomic analysis.** From top to bottom: PCA plot for the three cell lines; Heat map of grouped protein abundance of the 3 cell lines. Abundances were grouped and proteins were clustered by the Thermo Proteome Discoverer 3.1.1.93 software.

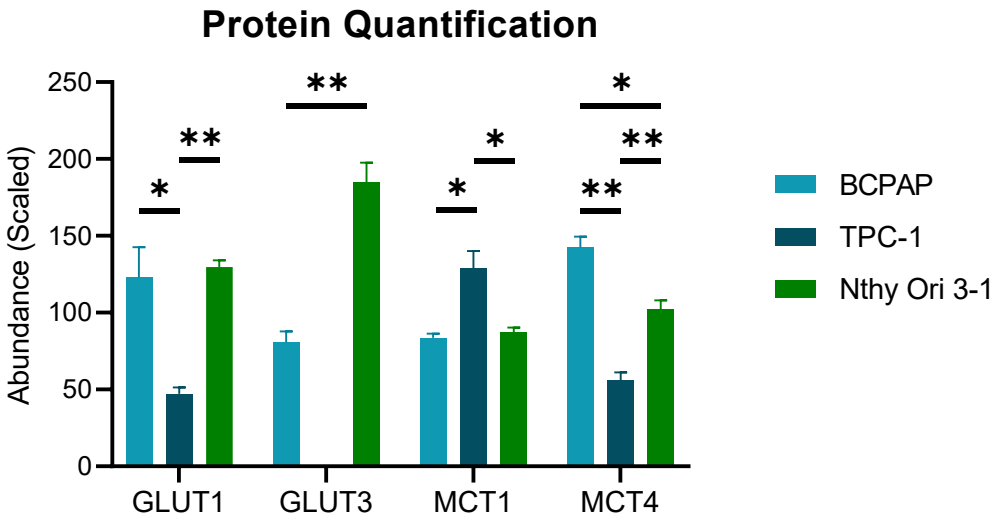

***Figure 10* – Absolute protein quantification graph (n=3).** Abundances were scaled by the Thermo Proteome Discoverer 3.1.1.93 software and statistical analysis was performed with GraphPad Prism Software version 8.0.1 (*, p<0.01; **, p<0.001).

Furthermore, full proteomic studies of the three cell lines were conducted. Table 3 compiles the information regarding the number of differently expressed proteins, number and name of the differently expressed cancer associated proteins and number of Gene Ontology biological processes and Reactome pathways enriched between cell lines and between both tumour cell lines versus the Nthy Ori 3-1 cell line. The differently expressed cancer associated proteins between one or both tumour cell lines and the Nthy Ori 3-1 cell line are presented in Figure 11.

Table 3. **Summary table of the gene enrichment proteomic analysis.** CA, cancer associated proteins. GO, Gene ontology

Comparisons	TPC-1		BCPAP		Nthy Ori 3-1		Cancer Cell Lines	
	BCPAP	Nthy Ori 3-1	TPC-1	Nthy Ori 3-1	TPC-1	BCPAP	Depleted	Enriched
Enriched Proteins	126	140	155	163	169	146	51	34
CA Proteins	3	2	9	5	13	13	10	0
Cancer Associated Proteins	ABL2 MAP2K4 NFIB	FAS RASA1	CCDC6 DDX10 FLI1 FSTL3 HMGA1 HMGA2 NUMA1 TNFAIP3	CD274 LCP1 SOX9 TBX3	ASPSCR1 CCDC6 PDAP1	MAP2K4 PDGFRB RHEB	B2M CD70 CDK4 CDKN2A CDKN2A COL1A1 COL5A1 HLA-A HLA-B TP53	
GO Biological Processes	13	10	10	8	5	10	1	0
Reactome Pathways	2	6	7	3	14	6	13	0

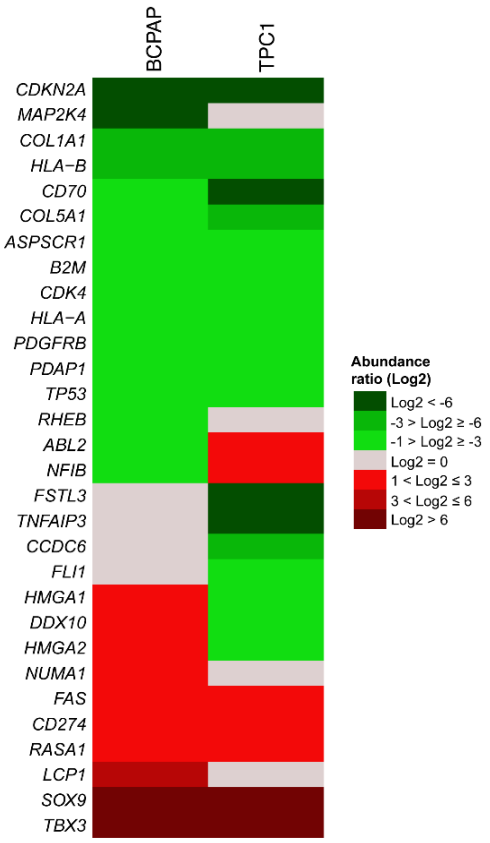

***Figure 11* – Abundance ratios of the differently expressed cancer associated proteins.** Values presented as ratio to Nthy Ori 3-1 protein abundance. Log2>6 indicates the protein was not expressed in Nthy Ori 3-1 cell line. Log2<6 indicates the protein was not expressed in the respective tumour cell line.

Comparison between the two tumour cell lines revealed that BCPAP cells exhibit enhanced viral defence mechanisms and increased fatty acid metabolic processes compared to TPC-1 cells. In contrast, TPC-1 cells are more active in the biosynthesis, transport, and metabolism of amino acids such as L-serine, methionine, and tyrosine, as well as in the metabolism of chemotherapeutic agents daunorubicin and doxorubicin (Figure 12).

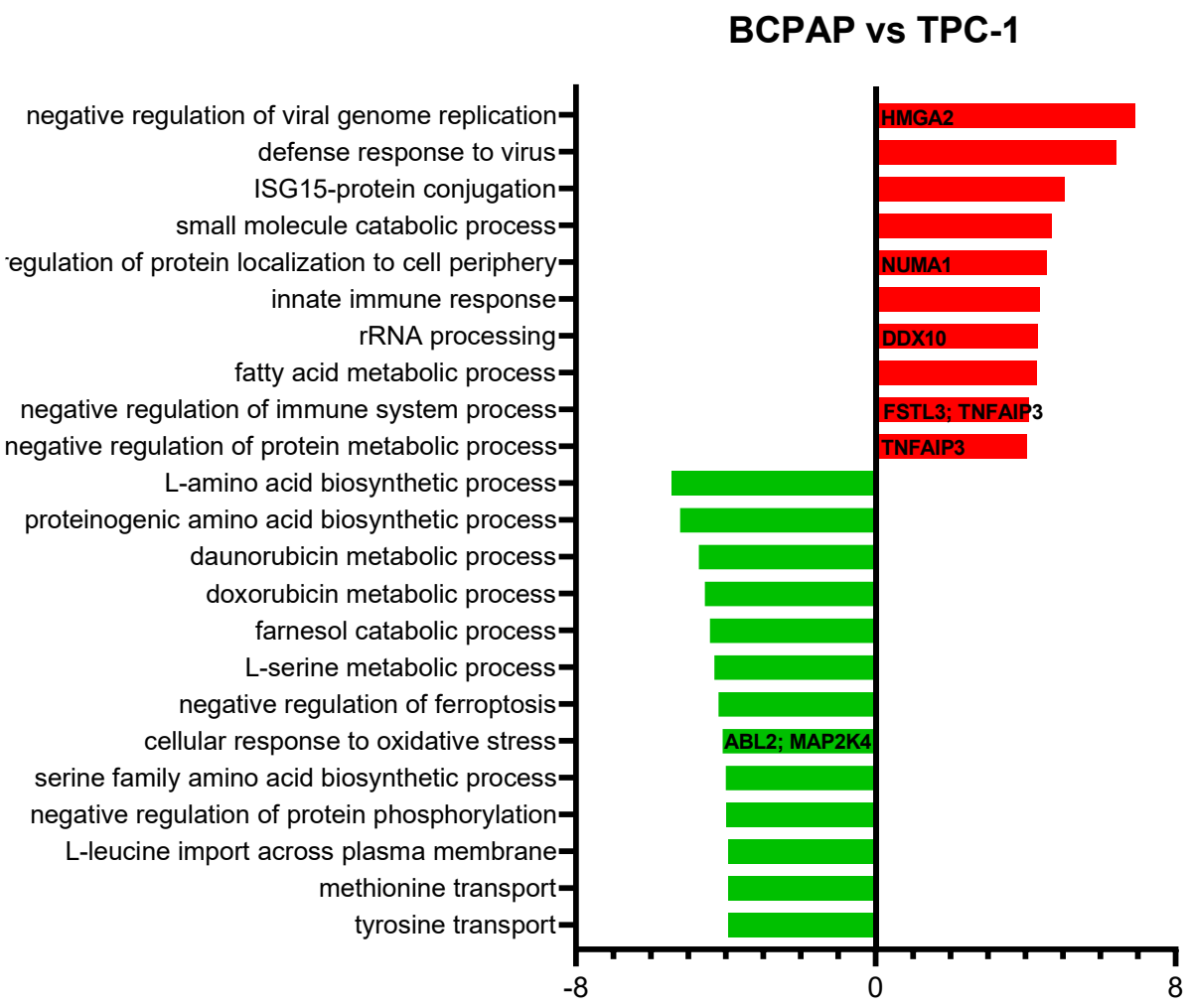

***Figure 12* – Gene Ontology biological processes and Reactome pathway analysis of enriched pathways between BCPAP and TPC-1 cell lines.** From top to bottom: Gene Ontology biological processes, Reactome pathways. Pathways sorted by lowest to highest p value. FDR<0.05. SAHF, senescence-associated heterochromatin foci.

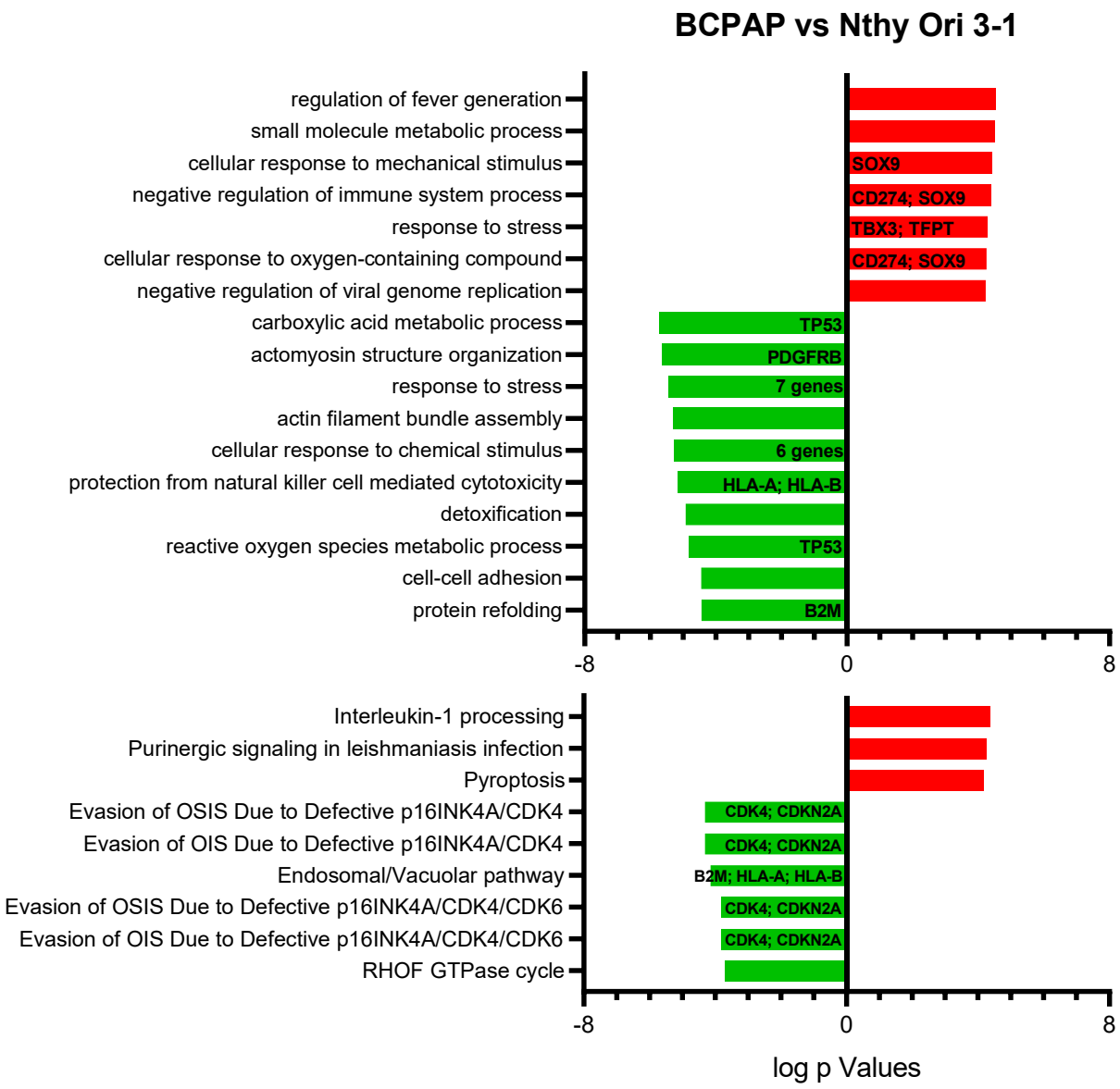

***Figure 13* - Gene Ontology biological processes and Reactome pathway analysis of enriched pathways between BCPAP and Nthy Ori 3-1 cell lines.** From top to bottom: Gene Ontology biological processes, Reactome pathways. Pathways sorted by lowest to highest p value. FDR<0.05. OSIS, oxidative stress induced senescence. OIS, oncogene induced senescence.

BCPAP cells are better prepared for small molecule metabolism, response to oxygen stress and inflammation and pyroptosis than Nthy Ori 3-1 cells (Figure 13). In contrast, TPC-1 cells exhibit higher expression of proteins involved in inflammatory responses and angiogenic pathways, as well as dysregulation of apoptotic processes (Figure 14).

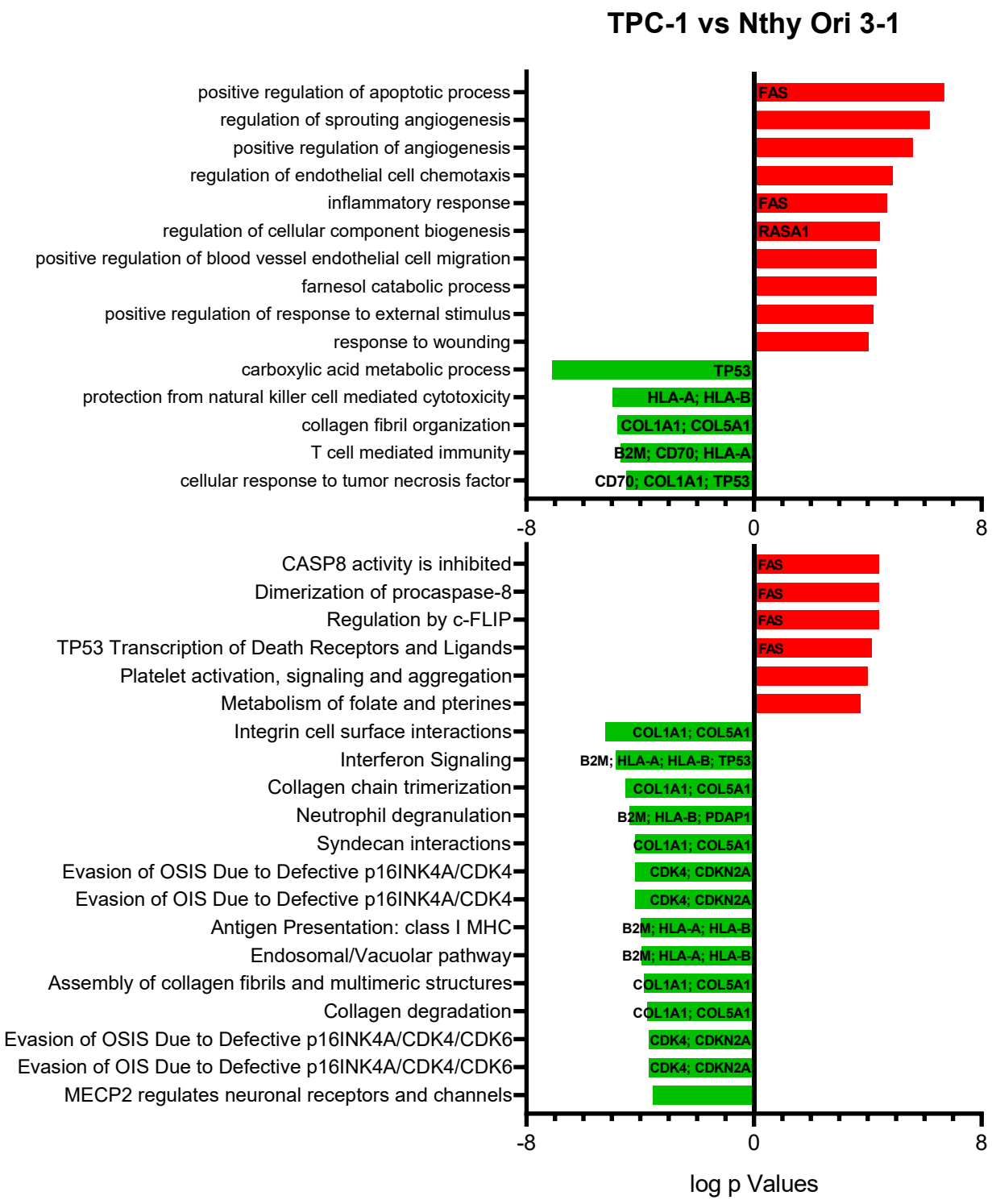

***Figure 14* - Gene Ontology biological processes and Reactome pathway analysis of enriched pathways between TPC-1 and Nthy Ori 3-1 cell lines.** From top to bottom: Gene Ontology biological processes, Reactome pathways. Pathways sorted by lowest to highest p value. FDR<0.05. OSIS, oxidative stress induced senescence. OIS, oncogene induced senescence.

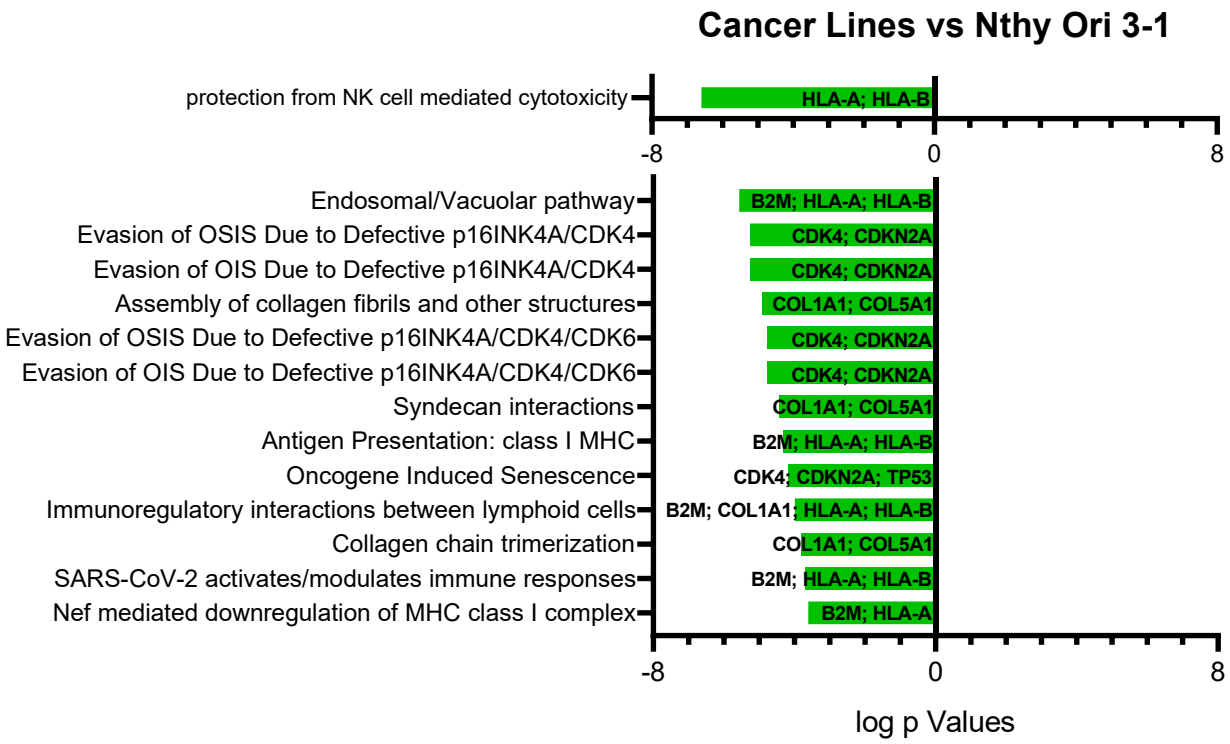

***Figure 15* - Gene Ontology biological processes and Reactome pathway analysis of enriched pathways between both tumour cell lines and Nthy Ori 3-1 cell line.** From top to bottom: Gene Ontology biological processes, Reactome pathways. Pathways sorted by lowest to highest p value. FDR<0.05. OSIS, oxidative stress induced senescence. OIS, oncogene induced senescence.

Despite not sharing any enriched pathway when comparing to the Nthy Ori 3-1 cell line, both tumour cell lines share a considerable amount of depleted pathways due to lack of expression of key cancer associated proteins, namely both cytoplasmatic and mitochondrial isoforms of cyclin-dependent kinase inhibitor 2A (CDKN2A), cyclin-dependent kinase 4 (CDK4), collagen type 1 alpha 1 and type 5 alpha 1 (COL1A1 and COL5A1), major histocompatibility complex, Class I, A and B (HLA-A and HLA-B), beta-2-microglobin (B2M), cluster of differentiation 70 (CD70) and tumour protein 53 (TP53). This causes the tumour cells to lose functions such as senescence evasion, endosomal regulation, assembly of collagen fibrils, class I MHC (major histocompatibility complex) presentation and protection against natural killer cells (Figure 15).

DISCUSSION

Discussion

Thyroid cancer is one of the fastest growing cancers in incidence in the last few decades, particularly the papillary thyroid cancer subtype (90). Although part of this increase can be attributed to overdiagnosis of small lesions, other risk factors have been suggested (91). One of the recently studied risk factors is metabolic diseases. Studies suggest that the concomitant increase of metabolic diseases, such as obesity and diabetes, may play a role in the increase of PTC incidence, since both have been described has risk factors for TC (7, 35).

Reprogramming of energy metabolism was firstly described as an emerging hallmark of cancer in 2011. In fact, Otto Warburg described as early as in 1930 alterations of cancer cell metabolism, namely the preference for aerobic glycolysis (92). Nowadays, more alterations to metabolic homeostasis have been described in cancer cells: deregulated uptake of glucose and amino acids, use of opportunistic modes of nutrient acquisition, use of glycolysis/TCA cycle intermediates for biosynthesis and NADPH production, increased demand for nitrogen, alterations in metabolite-driven gene regulation and metabolic interactions with the microenvironment (93).

Papillary thyroid cancer's most common genetic alterations, the *BRAF V600E*, Ras mutations and the *RET/PTC* fusions, all affect the MAPK pathway (11). MAPK induces a shift in cell metabolism through inactivation of AMPK, a key enzyme that also plays a role in the development of metabolic diseases (94). In fact, both metformin and canagliflozin, two drugs used for diabetes treatment, exert some of their effect by inducing AMPK expression, showing therapeutical potential for PTC treatment (65, 81).

In this context, the present study extends previous knowledge by directly characterizing the impact of metformin and canagliflozin on PTC cell metabolism. Specifically, we investigated their effects on glycolysis and cellular morphology, including mitochondrial number and morphology and endosomes and lipid droplets number, examined changes in glucose and lactate transporter expression, and performed a proteomic analysis to provide an integrated view of genetic-induced alterations in different cell lines. This approach allows us to discuss not only whether these agents influence PTC cell biology, but also how their metabolic actions may intersect with known oncogenic pathways.

Transmission electron microscopy (TEM) provided evidence that metabolic drugs exert distinct ultrastructural effects on thyroid cells. In TPC-1 cells, metformin treatment led to a modest increase in mitochondrial number, consistent with previous reports that complex I inhibition can trigger compensatory mitochondrial biogenesis in PTC (94). In BCPAP cells, however, metformin was associated with enlarged mitochondria, which may suggest defective mitophagy. This interpretation is supported by Thomas et al., who described impaired autophagic clearance of damaged mitochondria as a consequence of metabolic stress (95). The divergent mitochondrial responses between cell lines highlight the heterogeneity of PTC metabolic adaptation. Interestingly, canagliflozin induced a significant increase in total mitochondrial area in the non-tumoural Nthy Ori 3-1 line. This may reflect a stress response to reduced glucose

availability, as SGLT2 inhibition can impair glucose uptake and force mitochondrial compensation. Such findings raise the possibility that non-tumoural thyroid cells respond differently to metabolic perturbations, a factor that should be considered in translational contexts. Metformin also increased the number of endosomes in TPC-1 and Nthy Ori 3-1 cells. This aligns with experimental data from *C. elegans* and *Drosophila*, where metformin was shown to target an endosomal enzyme and thereby modulate the endocytic cycle (96). These alterations suggest that beyond its canonical mitochondrial effects, metformin may influence intracellular trafficking in thyroid cells. Finally, metformin treatment markedly increased the number of lipid droplets in all cell lines, particularly in the tumour-derived ones. This is a novel observation in the context of thyroid cancer, since previous work in rat adipose-derived stem cells reported that metformin inhibited lipid droplet fusion and growth (97). The opposite effect observed here may indicate a cancer-specific mechanism of lipid handling, possibly reflecting altered lipid storage as an adaptive strategy under metabolic stress. Further studies are warranted to clarify whether this phenotype represents an adaptive survival pathway or a vulnerability that could be therapeutically targeted.

The analysis of the glycolysis stress test revealed that treatment with both metformin and canagliflozin depleted the glycolytic reserve of all cells, particularly the tumour cell lines, since BCPAP and TPC-1 already prefer aerobic glycolysis due to the Warburg effect. Whilst these results are as expected for metformin treatment, since inhibition of the mitochondrial complex I inhibits oxidative phosphorylation and promotes the shift to glycolysis, which was already in action in the cancer cells, the same cannot be said about the canagliflozin results. The effects of canagliflozin were more unexpected. Given that this drug inhibits SGLT2-mediated glucose uptake, a decrease in glycolytic activity was anticipated. Instead, canagliflozin promoted a metabolic phenotype similar to that induced by metformin. One possible explanation is that SGLT2 inhibition triggers compensatory activation of alternative glucose transporters, allowing cells to sustain basal glycolysis while exhausting their capacity to further respond to energetic stress. Supporting this notion, previous studies have reported that canagliflozin can modulate AMPK signalling in PTC cells (81), potentially driving increased glycolytic flux despite reduced glucose entry through SGLT2.

Although immunofluorescence revealed the expression of all the transporters and co-transporter in study, the fact is that GLUT4 and SGLT2 were not detected and, subsequently, not quantified through Western Blot nor through LC-MS. This discrepancy may reflect low abundance of these proteins in thyroid cell lines, since both transporters have been previously reported in PTC patient samples (81, 95). However, data from *in vitro* models is scarce. Since GLUT4 delivery to the plasma membrane is mediated by insulin, this may contribute to physiological changes *in vivo* that we were not able to replicate in our cell lines (96).

The significant increase in MCT1 in the TPC-1 cell line, normally only seen in ATC, is associated with more aggressive tumours and may lead to increase in lactate uptake (22). On the other hand, GLUT1 and MCT4 expression, both associated with a more

aggressive biological subtype of TC, are downregulated in TPC-1 cells, limiting the glucose uptake rate and the lactate efflux rate, respectively (21, 97). Contrary to TPC-1, BCPAP cell line shows an increase in the expression of MCT4 comparing to the Nthy Ori 3-1 cell line, which leads to greater lactate efflux and tumour microenvironment acidification (22). However, GLUT3 expression is downregulated in BCPAP cells, suggesting that glucose intake in these cells is mediated by GLUT3 expression. Taken together, these findings highlight the heterogeneous metabolic adaptations of PTC cell lines, suggesting that distinct transporter expression patterns may underlie differences in glycolytic dependence, microenvironmental acidification, and ultimately, tumour aggressiveness.

The proteomic analysis by LC-MS identified a distinct expression profile between the papillary thyroid cancer cell lines (BCPAP and TPC-1) and the non-tumoural thyroid cell line (Nthy Ori 3-1). In total, several thousand proteins, were consistently quantified across replicates, with a subset showing significant differential expression.

When comparing *BRAF V600E*-mutated BCPAP cells to the *BRAF* wildtype TPC-1 cell line, there was a clear enrichment of several immune pathways, particularly those involving interferons and free fatty acid metabolism. In NIH3T3 mouse fibroblast cells transformed with *BRAF V600E*, the mutation was able to regulate the abundance of immunoregulatory lipids, playing a simultaneous immunological and metabolic regulatory role (98). On the other hand, TPC-1 cells overexpress proteins in many pathways regarding amino acid biosynthesis, transport and metabolism, fundamental activities that sustain its very fast proliferation rate.

Compared with Nthy Ori 3-1 cells, BCPAP cells display overexpression of immune pathways and stress response pathways, including responses to mechanical, oxidative and inflammatory stimuli, as well as pyroptosis. Pyroptosis is a form of programmed cell death that plays a role in the remodelling of the tumour microenvironment of PTCs, being proposed as a potential prognostic biomarker and therapy target (99).

TPC-1 cells present an overexpression of the FAS protein. This protein is part of the death receptor group of the tumour necrosis factor (TNF) receptor family and plays a pivotal role in apoptosis regulation, as can be seen by the multiple apoptosis-related pathways enriched in TPC-1 when compared to Nthy Ori 3-1 cells. In fact, there has been an association between activating mutations of the FAS gene and PTC development (100).

BCPAP and TPC-1 are depleted in several cancer associated proteins. Senescence pathways are dysregulated due to overexpression of CDKN2A and CDK4. Inhibition of CDK4 has been proven to induce senescence in other cancer types (101). This is especially important since CDKN2A is often found inactive in aggressive forms of differentiated thyroid cancer and in anaplastic thyroid cancer (102). Collagen fibrils assembly and chain trimerization were also disrupted. Whilst depleted in the tumoural cell lines, COL1A1 is associated with higher mortality in thyroid cancer, with expression levels reaching their highest for ATC and PDTC (103). Despite the downregulation of the expression of HLA-A and HLA-B, thyroid cancer cells remain protected from natural killer cells through the expression of immunosuppressive cells to the tumour

microenvironment. However, and with advances in the use of tumour microenvironment modulation for therapy purposes, this lack of defence against NK cells may be an important factor for PTC treatment (104). Lastly, the downregulation of TP53 in the TPC-1 cell line is interesting, since contrary to the BCPAP cell line, TPC-1 cells do not present any mutation on the gene (83, 84).

The results of this study reveal complex and heterogeneous metabolic adaptations in papillary thyroid cancer (PTC) cells in response to metformin and canagliflozin, highlighting the intersection between classical oncogenic pathways and metabolic alterations. Transmission electron microscopy showed an increase in mitochondrial number in TPC-1 cells and increased mitochondrial size in BCPAP cells after metformin treatment, suggesting differential responses to metabolic stress and potential autophagic dysfunction. Canagliflozin induced a significant increase in total mitochondrial area in Nthy Ori 3-1 cells, likely reflecting stress from decreased glucose uptake. Metformin also increased endosome numbers in TPC-1 and Nthy Ori 3-1 cells and lipid droplet accumulation particularly in tumour cell lines. Glycolysis stress tests revealed depletion of glycolytic reserve in all cells, notably BCPAP and TPC-1, with canagliflozin unexpectedly showing a similar effect to metformin. Analysis of transporters revealed heterogeneous expressions: GLUT1 and MCT4 downregulated in TPC-1, MCT1 upregulated in TPC-1, and MCT4 upregulated in BCPAP, reflecting diverse metabolic adaptations. Proteomic analysis showed *BRAF V600E*-mutated BCPAP cells enriched in immune and fatty acid pathways, while TPC-1 overexpressed amino acid biosynthesis and FAS-mediated apoptosis proteins. Both tumour lines were depleted in senescence-associated proteins and extracellular matrix components.

Together, these findings underscore the need to consider subtype- and drug-specific metabolic rewiring when evaluating metabolic therapies, as our observations of mitochondrial alterations, endosome and lipid droplet accumulation, and differential transporter expression reveal compensatory mechanisms that may modulate treatment efficacy.

CONCLUSION AND FUTURE PERSPECTIVES

Conclusion

This study provides novel insights into how anti-diabetic drugs can modulate the metabolism of papillary thyroid cancer (PTC) cells. Both metformin and canagliflozin induced important alterations in mitochondrial morphology, endosomal and lipid droplet dynamics, and glycolytic capacity, highlighting the presence of compensatory metabolic mechanisms. For the first time, a detailed analysis of glucose transporters, co-transporters, and monocarboxylate transporters in PTC cell lines revealed heterogeneous patterns that may support differences in glucose and lactate flux and tumor aggressiveness. Furthermore, proteomic profiling uncovered multiple pathways involved in metabolism, immune regulation, and stress responses, offering potential targets for diagnostic and therapeutic exploration.

In sum, our findings suggest that metformin and canagliflozin, while requiring further investigation, have the potential to modulate tumour cell metabolism and serve as potential co-adjuvant therapies for PTCs resistant to conventional treatments. However, a deeper understanding of the metabolic specificity of each tumour and of the compensatory mechanisms underlying the unexpected responses observed is necessary.

Future Perspectives

The relationship between cancer and metabolic diseases is a pivotal area of study in oncology in recent years. The complexity and variety of mechanisms by which metabolic disorders can affect multiple types of cancer directly and indirectly suggests that a lot of research is yet to be performed.

With the results of this study as a basis for progress, several other aims arise to be conducted in a near future, namely:

1. Conduct an immunoprecipitation assay for SGLT2. If expression is detected, follow with a SGLT2-mediated glucose uptake assay;
2. Assess the effects of metformin and canagliflozin on glucose uptake;
3. Conduct an immunofluorescence assay for detection of lipid droplets;
4. Expand the proteomic analysis of the cell lines for further integrated studies;
5. Investigate compensatory metabolic pathways activated in response to metformin and canagliflozin, including alternative glycolytic or lipid metabolism pathways;
6. Explore mitochondrial dynamics and autophagy regulation in response to these drugs, potentially using live-cell imaging or functional assays;
7. Validate in vitro findings using in vivo models or patient-derived organoids to assess translational relevance.

REFERENCES

References

1. Cheng F, Xiao J, Shao C, Huang F, Wang L, Ju Y, et al. Burden of Thyroid Cancer From 1990 to 2019 and Projections of Incidence and Mortality Until 2039 in China: Findings From Global Burden of Disease Study. Frontiers in Endocrinology. 2021;Volume 12 - 2021.

2. Bray F, Laversanne M, Sung H, Ferlay J, Siegel RL, Soerjomataram I, et al. Global cancer statistics 2022: GLOBOCAN estimates of incidence and mortality worldwide for 36 cancers in 185 countries. CA Cancer J Clin. 2024;74(3):229–63.

3. Li M, Dal Maso L, Pizzato M, Vaccarella S. Evolving epidemiological patterns of thyroid cancer and estimates of overdiagnosis in 2013–17 in 63 countries worldwide: a population-based study. The Lancet Diabetes & Endocrinology. 2024;12(11):824–36.

4. Seib CD, Sosa JA. Evolving Understanding of the Epidemiology of Thyroid Cancer. Endocrinology and Metabolism Clinics of North America. 2019;48(1):23–35.

5. Kitahara CM, Schneider AB. Epidemiology of Thyroid Cancer. Cancer Epidemiol Biomarkers Prev. 2022;31(7):1284–97.

6. Kitahara CM, D KRF, Jørgensen JOL, Cronin-Fenton D, Sørensen HT. Benign Thyroid Diseases and Risk of Thyroid Cancer: A Nationwide Cohort Study. J Clin Endocrinol Metab. 2018;103(6):2216–24.

7. Kitahara CM, McCullough ML, Franceschi S, Rinaldi S, Wolk A, Neta G, et al. Anthropometric Factors and Thyroid Cancer Risk by Histological Subtype: Pooled Analysis of 22 Prospective Studies. Thyroid. 2016;26(2):306–18.

8. Lauby-Secretan B, Scoccianti C, Loomis D, Grosse Y, Bianchini F, Straif K. Body Fatness and Cancer--Viewpoint of the IARC Working Group. N Engl J Med. 2016;375(8):794–8.

9. Damstra T, Barlow S, Bergman A, Kavlock R, de la Salut OM. Global Assessment of the State-of-the-science of Endocrine Disruptor. 2002.

10. Alsen M, Sinclair C, Cooke P, Ziadkhanpour K, Genden E, van Gerwen M. Endocrine Disrupting Chemicals and Thyroid Cancer: An Overview. Toxics. 2021;9(1).

11. Prete A, Borges de Souza P, Censi S, Muzza M, Nucci N, Sponziello M. Update on Fundamental Mechanisms of Thyroid Cancer. Frontiers in Endocrinology. 2020;Volume 11 - 2020.

12. Chen DW, Lang BHH, McLeod DSA, Newbold K, Haymart MR. Thyroid cancer. Lancet. 2023;401(10387):1531–44.

13. Ali SZ, Baloch ZW, Cochand-Priollet B, Schmitt FC, Vielh P, VanderLaan PA. The 2023 Bethesda System for Reporting Thyroid Cytopathology. Thyroid. 2023;33(9):1039–44.

14. Díaz Vico T, Martínez-Amores Martínez B, Mihic Góngora L, Jiménez-Fonseca P, Peinado Martín P, Grao Torrente I, et al. Systemic Therapeutic Options in Radioiodine-Refractory Differentiated Thyroid Cancer: Current Indications and Optimal Timing. Cancers (Basel). 2025;17(11).

15. Liu R, Xing M. TERT promoter mutations in thyroid cancer. Endocr Relat Cancer. 2016;23(3):R143–55.

16. Integrated genomic characterization of papillary thyroid carcinoma. Cell. 2014;159(3):676–90.

17. Soares P, Póvoa AA, Melo M, Vinagre J, Máximo V, Eloy C, et al. Molecular Pathology of Non-familial Follicular Epithelial–Derived Thyroid Cancer in Adults: From RAS/BRAF-like Tumor Designations to Molecular Risk Stratification. Endocrine Pathology. 2021;32(1):44–62.

18. Qu N, Chen D, Ma B, Zhang L, Wang Q, Wang Y, et al. Integrated proteogenomic and metabolomic characterization of papillary thyroid cancer with different recurrence risks. Nature Communications. 2024;15(1):3175.

19. Koppenol WH, Bounds PL, Dang CV. Otto Warburg's contributions to current concepts of cancer metabolism. Nature Reviews Cancer. 2011;11(5):325–37.

20. Wan Y, Li G, Cui G, Duan S, Chang S. Reprogramming of Thyroid Cancer Metabolism: from Mechanism to Therapeutic Strategy. Molecular Cancer. 2025;24(1):74.

21. Heydarzadeh S, Moshtaghie AA, Daneshpoor M, Hedayati M. Regulators of glucose uptake in thyroid cancer cell lines. Cell Communication and Signaling. 2020;18(1):83.

22. Gill KS, Tassone P, Hamilton J, Hjelm N, Luginbuhl A, Cognetti D, et al. Thyroid Cancer Metabolism: A Review. J Thyroid Disord Ther. 2016;5(1).

23. Ban EJ, Kim D, Kim JK, Kang SW, Lee J, Jeong JJ, et al. Lactate Dehydrogenase A as a Potential New Biomarker for Thyroid Cancer. Endocrinol Metab (Seoul). 2021;36(1):96–105.

24. Gao Y, Yang F, Yang XA, Zhang L, Yu H, Cheng X, et al. Mitochondrial metabolism is inhibited by the HIF1α-MYC-PGC-1β axis in BRAF V600E thyroid cancer. Febs j. 2019;286(7):1420–36.

25. Zhang H, Zhou X-D, Shapiro MD, Lip GYH, Tilg H, Valenti L, et al. Global burden of metabolic diseases, 1990–2021. Metabolism - Clinical and Experimental. 2024;160.

26. Harborg S, Kjærgaard KA, Thomsen RW, Borgquist S, Cronin-Fenton D, Hjorth CF. New Horizons: Epidemiology of Obesity, Diabetes Mellitus, and Cancer Prognosis. The Journal of Clinical Endocrinology & Metabolism. 2023;109(4):924–35.

27. Abiri B, Ahmadi AR, Valizadeh A, Abbaspour F, Valizadeh M, Hedayati M. Obesity and thyroid cancer: unraveling the connection through a systematic review and meta-analysis of cohort studies. J Diabetes Metab Disord. 2024;23(1):461–74.

28. Kitahara CM, Pfeiffer RM, Sosa JA, Shiels MS. Impact of Overweight and Obesity on US Papillary Thyroid Cancer Incidence Trends (1995-2015). J Natl Cancer Inst. 2020;112(8):810–7.

29. Rahman ST, Pandeya N, Neale RE, McLeod DSA, Bain CJ, Baade PD, et al. Obesity Is Associated with BRAF(V600E)-Mutated Thyroid Cancer. Thyroid. 2020;30(10):1518–27.

30. Kim WG, Cheng SY. Mechanisms Linking Obesity and Thyroid Cancer Development and Progression in Mouse Models. Horm Cancer. 2018;9(2):108–16.

31. Wang Q, Li J, Qiao H, Zhang Y, Xu Y, Chen R, et al. Metabolic syndrome and cancer risk: A bidirectional two-sample Mendelian randomization study. Experimental Gerontology. 2025;207:112802.

32. Alves R, Santos AJ, Kislaya I, Nunes B, Freire AC. Metabolic Syndrome in Portugal: Prevalence and Associated Factors. Acta Médica Portuguesa. 2022;35(9):633–43.

33. Fahed G, Aoun L, Bou Zerdan M, Allam S, Bou Zerdan M, Bouferraa Y, et al. Metabolic Syndrome: Updates on Pathophysiology and Management in 2021. International Journal of Molecular Sciences [Internet]. 2022; 23(2).

34. Yin DT, He H, Yu K, Xie J, Lei M, Ma R, et al. The association between thyroid cancer and insulin resistance, metabolic syndrome and its components: A systematic review and meta-analysis. Int J Surg. 2018;57:66–75.

35. Wu R, Zhang J, Zou G, Li S, Wang J, Li X, et al. Diabetes Mellitus and Thyroid Cancers: Risky Correlation, Underlying Mechanisms and Clinical Prevention. Diabetes, Metabolic Syndrome and Obesity. 2024;17(null):809–23.

36. Srivastava SP, Goodwin JE. Cancer Biology and Prevention in Diabetes. Cells. 2020;9(6).

37. Aschebrook-Kilfoy B, Sabra MM, Brenner A, Moore SC, Ron E, Schatzkin A, et al. Diabetes and thyroid cancer risk in the National Institutes of Health-AARP Diet and Health Study. Thyroid. 2011;21(9):957–63.

38. Linkeviciute-Ulinskiene D, Patasius A, Zabuliene L, Stukas R, Smailyte G. Increased Risk of Site-Specific Cancer in People with Type 2 Diabetes: A National Cohort Study. Int J Environ Res Public Health. 2019;17(1).

39. Yeo Y, Ma SH, Hwang Y, Horn-Ross PL, Hsing A, Lee KE, et al. Diabetes mellitus and risk of thyroid cancer: a meta-analysis. PLoS One. 2014;9(6):e98135.

40. Zhan YS, Feng L, Tang SH, Li WG, Xu M, Liu TF, et al. Glucose metabolism disorders in cancer patients in a Chinese population. Med Oncol. 2010;27(2):177–84.

41. Seo YG, Choi HC, An AR, Park DJ, Park YJ, Lee KE, et al. The Association between Type 2 Diabetes Mellitus and Thyroid Cancer. J Diabetes Res. 2017;2017:5850879.

42. Carstensen B, Read SH, Friis S, Sund R, Keskimäki I, Svensson AM, et al. Cancer incidence in persons with type 1 diabetes: a five-country study of 9,000 cancers in type 1 diabetic individuals. Diabetologia. 2016;59(5):980–8.

43. Li H, Qian J. Association of diabetes mellitus with thyroid cancer risk: A meta-analysis of cohort studies. Medicine (Baltimore). 2017;96(47):e8230.

44. Dong WW, Zhang DL, Wang ZH, Lv CZ, Zhang P, Zhang H. Different types of diabetes mellitus and risk of thyroid cancer: A meta-analysis of cohort studies. Front Endocrinol (Lausanne). 2022;13:971213.

45. Saewai C, Fumaneeshoat O, Thongsuksai P, Ingviya T. Diabetes Mellitus as Cancer Risk: A 14-year, Cross-Sectional Analysis. Nutr Cancer. 2023;75(6):1454–63.

46. Hu Y, Zhang X, Ma Y, Yuan C, Wang M, Wu K, et al. Incident Type 2 Diabetes Duration and Cancer Risk: A Prospective Study in Two US Cohorts. J Natl Cancer Inst. 2021;113(4):381–9.

47. Poor glycemic control is associated with the risk of subclinical hypothyroidism in patients with type 2 diabetes mellitus FAU - Cho, Jae Ho FAU - Kim, Ho Jin FAU - Lee, Jun Ho FAU - Park,

Il Rae FAU - Moon, Jun Sung FAU - Yoon, Ji Sung FAU - Lee, In-Kyu FAU - Won, Kyu Chang FAU - Lee, Hyoung Woo. Korean J Intern Med. 2016;31(4):703–11.

48. Xu B, Gu SY, Zhou NM, Jiang JJ. Association between thyroid stimulating hormone levels and papillary thyroid cancer risk: A meta-analysis. Open Life Sci. 2023;18(1):20220671.

49. Zou M, Baitei EY, Al-Rijjal RA, Parhar RS, Al-Mohanna FA, Kimura S, et al. TSH overcomes BrafV600E-induced senescence to promote tumor progression via downregulation of p53 expression in papillary thyroid cancer. Oncogene. 2016;35(15):1909–18.

50. Song YS, Kim MJ, Sun HJ, Kim HH, Shin HS, Kim YA, et al. Aberrant Thyroid-Stimulating Hormone Receptor Signaling Increases VEGF-A and CXCL8 Secretion of Thyroid Cancer Cells, Contributing to Angiogenesis and Tumor Growth. Clinical Cancer Research. 2019;25(1):414–25.

51. Tabur S, Aksoy ŞN, Korkmaz H, Ozkaya M, Aksoy N, Akarsu E. Investigation of the role of 8-OHdG and oxidative stress in papillary thyroid carcinoma. Tumor Biology. 2015;36(4):2667–74.

52. Zhang Z, Xu T, Qin W, Huang B, Chen W, Li S, et al. Upregulated PTPN2 induced by inflammatory response or oxidative stress stimulates the progression of thyroid cancer. Biochemical and Biophysical Research Communications. 2020;522(1):21–5.

53. Wang Z, Li J, Liu Z, Yue L. Nrf2 as a novel diagnostic biomarker for papillary thyroid carcinoma. Eur J Histochem. 2023;67(2).

54. Masenga SK, Kabwe LS, Chakulya M, Kirabo A. Mechanisms of Oxidative Stress in Metabolic Syndrome. International Journal of Molecular Sciences. 2023;24(9):7898.

55. Manzella L, Massimino M, Stella S, Tirrò E, Pennisi MS, Martorana F, et al. Activation of the IGF Axis in Thyroid Cancer: Implications for Tumorigenesis and Treatment. International Journal of Molecular Sciences. 2019;20(13):3258.

56. Dilworth L, Facey A, Omoruyi F. Diabetes Mellitus and Its Metabolic Complications: The Role of Adipose Tissues. Int J Mol Sci. 2021;22(14).

57. Uddin S, Bavi P, Siraj AK, Ahmed M, Al-Rasheed M, Hussain AR, et al. Leptin-R and its association with PI3K/AKT signaling pathway in papillary thyroid carcinoma. Endocrine-Related Cancer. 2010;17(1):191–202.

58. Zhou Y, Yang Y, Zhou T, Li B, Wang Z. Adiponectin and Thyroid Cancer: Insight into the Association between Adiponectin and Obesity. Aging Dis. 2021;12(2):597–613.

59. Nigro E, Orlandella FM, Polito R, Mariniello RM, Monaco ML, Mallardo M, et al. Adiponectin and leptin exert antagonizing effects on proliferation and motility of papillary thyroid cancer cell lines. Journal of Physiology and Biochemistry. 2021;77(2):237–48.

60. Balaky HM, Ismail PA. Serum resistin, visfatin, IL-17 and IL-23 as novel diagnostic biomarkers for thyroid carcinoma. AIMS Allergy and Immunology. 2025;9(3):166–79.

61. Zhang X, Li S, Wang J, Liu F, Zhao Y. Relationship Between Serum Inflammatory Factor Levels and Differentiated Thyroid Carcinoma. Technology in Cancer Research & Treatment. 2021;20:1533033821990055.

62. Zhang L, Xu S, Cheng X, Wu J, Wang Y, Gao W, et al. Inflammatory tumor microenvironment of thyroid cancer promotes cellular dedifferentiation and silencing of iodide-handling genes expression. Pathology - Research and Practice. 2023;246:154495.

63. Zhao J, Wen J, Wang S, Yao J, Liao L, Dong J. Association between adipokines and thyroid carcinoma: a meta-analysis of case-control studies. BMC Cancer. 2020;20(1):788.

64. Greco A, Coperchini F, Croce L, Magri F, Teliti M, Rotondi M. Drug repositioning in thyroid cancer treatment: the intriguing case of anti-diabetic drugs. Front Pharmacol. 2023;14:1303844.

65. Lv Z, Guo Y. Metformin and Its Benefits for Various Diseases. Frontiers in Endocrinology. 2020;Volume 11 - 2020.

66. Li H, Chen Y, Hu L, Yang W, Gao Z, Liu M, et al. Will metformin use lead to a decreased risk of thyroid cancer? A systematic review and meta-analyses. European Journal of Medical Research. 2023;28(1):392.

67. Wincenciuk K, Buczyńska A, Krętowski AJ, Adamska A. Metformin as a promising therapeutic agent for papillary thyroid cancer: Mechanisms of antitumor and pro-apoptotic activity. Translational Oncology. 2025;60:102483.

68. Chen G, Xu S, Renko K, Derwahl M. Metformin Inhibits Growth of Thyroid Carcinoma Cells, Suppresses Self-Renewal of Derived Cancer Stem Cells, and Potentiates the Effect of Chemotherapeutic Agents. The Journal of Clinical Endocrinology & Metabolism. 2012;97(4):E510–E20.

69. Cho SW, Yi KH, Han SK, Sun HJ, Kim YA, Oh B-C, et al. Therapeutic potential of metformin in papillary thyroid cancer in vitro and in vivo. Molecular and Cellular Endocrinology. 2014;393(1):24–9.

70. Klubo-Gwiezdzinska J, Costello J, Jr, Patel A, Bauer A, Jensen K, Mete M, et al. Treatment With Metformin Is Associated With Higher Remission Rate in Diabetic Patients With Thyroid Cancer. The Journal of Clinical Endocrinology & Metabolism. 2013;98(8):3269–79.

71. Ye J, Qi L, Chen K, Li R, Song S, Zhou C, et al. Metformin induces TPC-1 cell apoptosis through endoplasmic reticulum stress-associated pathways in vitro and in vivo. Int J Oncol. 2019;55(1):331–9.

72. He Y, Cao L, Wang L, Liu L, Huang Y, Gong X. Metformin Inhibits Proliferation of Human Thyroid Cancer TPC-1 Cells by Decreasing LRP2 to Suppress the JNK Pathway. Onco Targets Ther. 2020;13:45–50.

73. Thakur S, Daley B, Gaskins K, Vasko VV, Boufraqech M, Patel D, et al. Metformin Targets Mitochondrial Glycerophosphate Dehydrogenase to Control Rate of Oxidative Phosphorylation and Growth of Thyroid Cancer In Vitro and In Vivo. Clinical Cancer Research. 2018;24(16):4030–43.

74. Yu Y, Feng C, Kuang J, Guo L, Guan H. Metformin exerts an antitumoral effect on papillary thyroid cancer cells through altered cell energy metabolism and sensitized by BACH1 depletion. Endocrine. 2022;76(1):116–31.

75. Shen C-T, Wei W-J, Qiu Z-L, Song H-J, Zhang X-Y, Sun Z-K, et al. Metformin reduces glycometabolism of papillary thyroid carcinoma in vitro and in vivo. Journal of Molecular Endocrinology. 2017;58(1):15–23.

76. Bikas A, Jensen K, Patel A, Costello J, McDaniel D, Klubo-Gwiezdzinska J, et al. Glucose-deprivation increases thyroid cancer cells sensitivity to metformin. Endocrine-Related Cancer. 2015;22(6):919–32.

77. Ouyang J, Feng Y, Zhang Y, Liu Y, Li S, Wang J, et al. Integration of metabolomics and transcriptomics reveals metformin suppresses thyroid cancer progression via inhibiting glycolysis and restraining DNA replication. Biomedicine & Pharmacotherapy. 2023;168:115659.

78. Kheder S, Sisley K, Hadad S, Balasubramanian SP. Effects of prolonged exposure to low dose metformin in thyroid cancer cell lines. J Cancer. 2017;8(6):1053–61.

79. Tentolouris A, Vlachakis P, Tzeravini E, Eleftheriadou I, Tentolouris N. SGLT2 Inhibitors: A Review of Their Antidiabetic and Cardioprotective Effects. International Journal of Environmental Research and Public Health. 2019;16(16):2965.

80. Dutka M, Bobiński R, Francuz T, Garczorz W, Zimmer K, Ilczak T, et al. SGLT-2 Inhibitors in Cancer Treatment—Mechanisms of Action and Emerging New Perspectives. Cancers. 2022;14(23):5811.

81. Wang Y, Yang L, Mao L, Zhang L, Zhu Y, Xu Y, et al. SGLT2 inhibition restrains thyroid cancer growth via G1/S phase transition arrest and apoptosis mediated by DNA damage response signaling pathways. Cancer Cell International. 2022;22(1):74.

82. Coperchini F, Greco A, Croce L, Pignatti P, Muzza M, Petrosino E, et al. Canagliflozin reduces thyroid cancer cells migration in vitro by inhibiting CXCL8 and CCL2: An additional anti-tumor effect of the drug. Biomedicine & Pharmacotherapy. 2024;170:115974.

83. Saiselet M, Floor S, Tarabichi M, Dom G, Hébrant A, van Staveren W, et al. Thyroid cancer cell lines: an overview. Frontiers in Endocrinology. 2012;Volume 3 - 2012.

84. Landa I, Pozdeyev N, Korch C, Marlow LA, Smallridge RC, Copland JA, et al. Comprehensive Genetic Characterization of Human Thyroid Cancer Cell Lines: A Validated Panel for Preclinical Studies. Clin Cancer Res. 2019;25(10):3141–51.

85. Verheijen M, Lienhard M, Schrooders Y, Clayton O, Nudischer R, Boerno S, et al. DMSO induces drastic changes in human cellular processes and epigenetic landscape in vitro. Scientific Reports. 2019;9(1):4641.

86. Osório H, Silva C, Ferreira M, Gullo I, Máximo V, Barros R, et al. Proteomics Analysis of Gastric Cancer Patients with Diabetes Mellitus. J Clin Med. 2021;10(3).

87. Thomas PD, Ebert D, Muruganujan A, Mushayahama T, Albou L-P, Mi H. PANTHER: Making genome-scale phylogenetics accessible to all. Protein Science. 2022;31(1):8–22.

88. Consortium TGO, Aleksander SA, Balhoff J, Carbon S, Cherry JM, Drabkin HJ, et al. The Gene Ontology knowledgebase in 2023. Genetics. 2023;224(1).

89. Ashburner M, Ball CA, Blake JA, Botstein D, Butler H, Cherry JM, et al. Gene Ontology: tool for the unification of biology. Nature Genetics. 2000;25(1):25–9.

90. Weller S, Chu C, Lam AK. Assessing the Rise in Papillary Thyroid Cancer Incidence: A 38-Year Australian Study Investigating WHO Classification Influence. J Epidemiol Glob Health. 2025;15(1):9.

91. Hajeer MH, Awad HA, Abdullah NI, Almuhaisen GH, Abudalu LE. The rising trend in papillary thyroid carcinoma. True increase or over diagnosis? Saudi Med J. 2018;39(2):147–53.

92. Hanahan D, Weinberg Robert A. Hallmarks of Cancer: The Next Generation. Cell. 2011;144(5):646–74.

93. Pavlova NN, Thompson CB. The Emerging Hallmarks of Cancer Metabolism. Cell Metab. 2016;23(1):27–47.

94. Yuan J, Dong X, Yap J, Hu J. The MAPK and AMPK signalings: interplay and implication in targeted cancer therapy. Journal of Hematology & Oncology. 2020;13(1):113.

95. Kaida H, Hiromatsu Y, Kurata S, Kawahara A, Hattori S, Taira T, et al. Relationship between clinicopathological factors and fluorine-18-fluorodeoxyglucose uptake in patients with papillary thyroid cancer. Nuclear Medicine Communications. 2011;32(8):690–8.

96. Koester AM, Geiser A, Bowman PRT, van de Linde S, Gadegaard N, Bryant NJ, et al. GLUT4 translocation and dispersal operate in multiple cell types and are negatively correlated with cell size in adipocytes. Scientific Reports. 2022;12(1):20535.

97. Kim CA, Yoo J, Lee WK, Song DE, Kim WG, Jeon MJ. Monocarboxylate Transporter 4 Expression in Thyroid Cancer. Int J Thyroidol. 2024;17(2):272–6.

98. Turner JA, Paton EL, Van Gulick R, Stefanoni D, Cendali F, Reisz J, et al. BRAF Modulates Lipid Use and Accumulation. Cancers (Basel). 2022;14(9).

99. Li F, Du R, Kou J, Li J, Zhou L, Zhang D, et al. Elucidating the role of Pyroptosis in papillary thyroid cancer: prognostic, immunological, and therapeutic perspectives. Cancer Cell Int. 2024;24(1):45.

100. Eun YG, Lee YC, Kim SK, Chung J-H, Kwon KH, Park IS. Single nucleotide polymorphisms of the Fas gene are associated with papillary thyroid cancer. Auris Nasus Larynx. 2015;42(4):326–31.

101. Wang L, Lankhorst L, Bernards R. Exploiting senescence for the treatment of cancer. Nature Reviews Cancer. 2022;22(6):340–55.

102. Pakkianathan J, Yamauchi CR, Barseghyan L, Cruz J, Simental AA, Khan S. Mutational Landmarks in Anaplastic Thyroid Cancer: A Perspective of a New Treatment Strategy. Journal of Clinical Medicine. 2025;14(9):2898.

103. Jolly LA, Novitskiy S, Owens P, Massoll N, Cheng N, Fang W, et al. Fibroblast-Mediated Collagen Remodeling Within the Tumor Microenvironment Facilitates Progression of Thyroid Cancers Driven by BrafV600E and Pten Loss. Cancer Res. 2016;76(7):1804–13.

104. Prakash K, Rajendran RL, Dhayalan S, Gangadaran P, Ahn B-C, Aruljothi KN. Natural Killer Cell and Extracellular Vesicle-Based Immunotherapy in Thyroid Cancer: Advances, Challenges, and Future Perspectives. Cells. 2025;14(14):1087.

SUPPLEMENTARY DATA

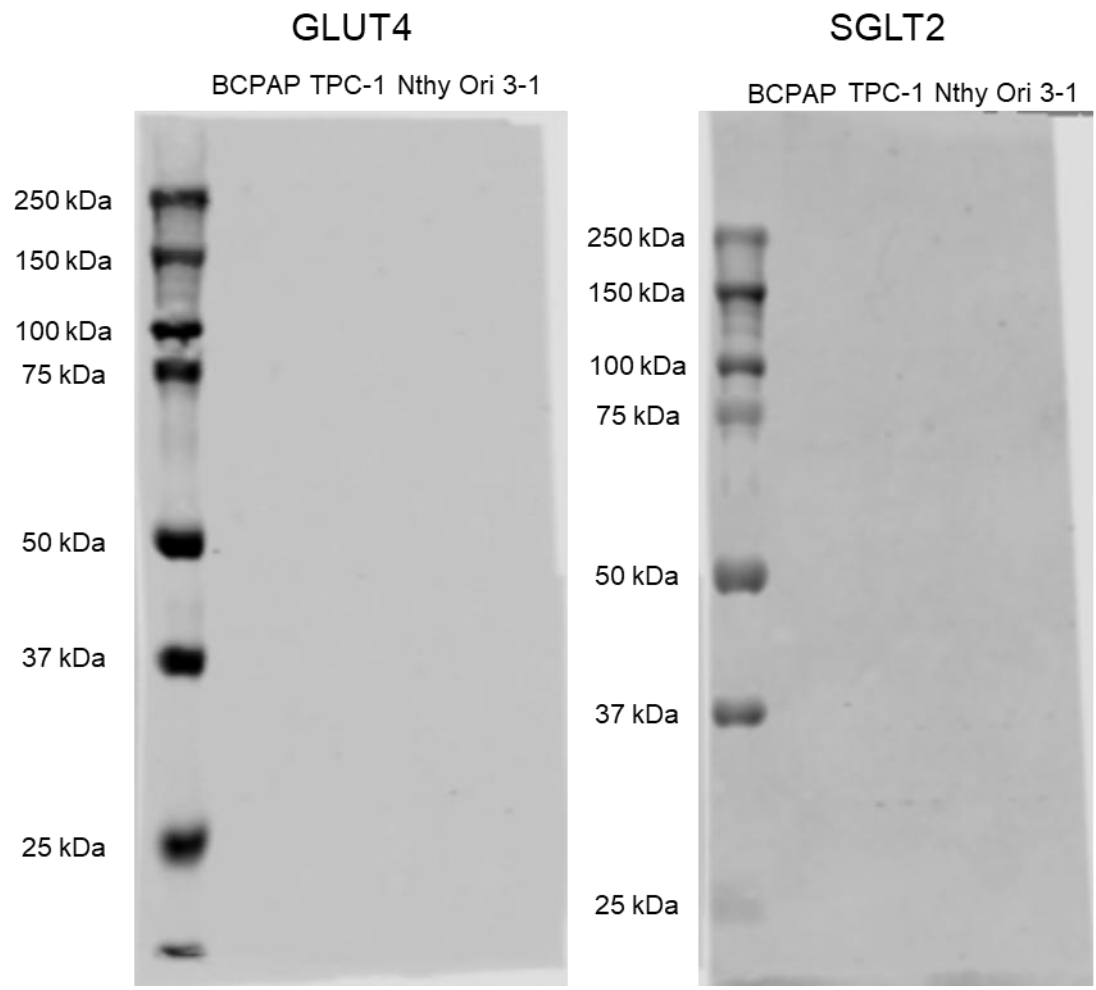

***Supplementary Figure 1* - Western Blot membrane images.** From left to right: GLUT4, SGLT2. Membranes revealed with Odyssey ® CLx Infrared Imaging System at 800 nm.

FACULDADE DE **MEDICINA**